

UNIVERSITY OF CALGARY

Decision Feedback Equalizer for Multiple-Input Multiple-Output Wireless Systems

by

Lin Wang

A THESIS

SUBMITTED TO THE FACULTY OF GRADUATE STUDIES

IN PARTIAL FULFILMENT OF THE REQUIREMENTS FOR THE

DEGREE OF MASTER OF SCIENCE

DEPARTMENT OF ELECTRICAL AND COMPUTER ENGINEERING

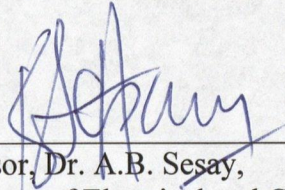
CALGARY, ALBERTA

FEBRUARY, 2007

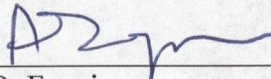
© Lin Wang 2007

THE UNIVERSITY OF CALGARY
FACULTY OF GRADUATE STUDIES

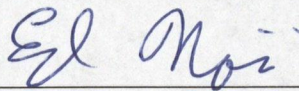
The undersigned certify that they have read, and recommend to the Faculty of Graduate Studies for acceptance, a thesis entitled, "Decision Feedback Equalizer for Multiple-Input Multiple-Output Wireless Systems" submitted by Lin Wang in partial fulfillment of the requirements for the degree of Master of Science.



Supervisor, Dr. A.B. Sesay,
Department of Electrical and Computer Engineering.



Dr. A.O. Fapojuwo,
Department of Electrical and Computer Engineering.



Dr. E. Nowicki,
Department of Electrical and Computer Engineering.



Dr. Y. Gao,
Dept of Geomatics Engineering.

Jan 19, 2007

Date

ABSTRACT

This thesis focuses on the decision feedback equalization (DFE) technique in multiple-input multiple-output (MIMO) wireless channels. In MIMO channels, the distortions in the transmitted signals are mainly due to inter-symbol interference (ISI). Equalization techniques help to recover the original transmitted signals by relieving ISI. DFE has higher effectiveness than linear equalizers. Comparing to the other nonlinear equalizers, DFE has lower computation complexity.

Space-time coding is a technology with which full diversity gain can be obtained in MIMO channels. In this thesis, combined with space-time block codes (STBC), two STBC-DFE schemes are proposed. These two schemes are further combined with convolutional codes to improve the performance. The performances of these schemes are also compared with that of orthogonal frequency division multiplexing (OFDM) system which is another advanced anti-ISI technology. Computer simulation results show that the presented schemes are potential solutions for the third generation wireless communications.

ACKNOWLEDGEMENTS

I wish to offer my sincere thanks to all those who contribute to this thesis either through their ideas or their work. Among all the people who have helped me in completing this thesis, I would like to call special attention to the following people for the importance of their contributions:

Dr. Abu Sesay – my dear supervisor, for having guided me along the research path and for proofing this text.

Mr. Feng Zhang – my dear friend, for his dedicated effort in giving advices and cooperating in this project.

Miss Youlan Li – my dear friend, for prior discussion of text.

My dear parents for their consistent effort in encouraging me to overcome the difficulties from the very beginning of my master studies.

TABLE OF CONTENTS

Approval Page.....	ii
Abstract.....	iii
Acknowledgements.....	iv
Table of Contents.....	v
List of Table	vii
List of Figures and Illustrations	viii
CHAPTER ONE: INTRODUCTION.....	1
CHAPTER TWO: SISO-DFE SYSTEM AND MIMO-DFE SYSTEM.....	7
2.1 SISO-DFE System.....	10
2.2 Multiple-Input Multiple-Output Rayleigh fading channel.....	12
2.3 MIMO-DFE System	12
2.4 Computer Simulations and Analysis.....	15
2.5 Chapter Summary	16
CHAPTER THREE: CONCATENATION OF SPACE-TIME BLOCK CODING AND DECISION FEEDBACK EQUALIZER.....	17
3.1 Encoding and Decoding of Space-Time Coding	18
3.2 Space-Time Block Coding.....	19
3.3 Other Space-Time Codes.....	22
3.4 STBC-DFE Scheme Structure	22
3.4.1 DFE for Multi-user Case One.....	22
3.4.2 DFE for Multi-user Case Two	24
3.4.3 Structure of STBC-DFE	25
3.5 Computer Simulations and Analysis.....	28
3.5.1 STBC-DFE for Multi-User Case One	28
3.5.2 STBC-DFE for Multi-User Case Two.....	31
3.6 Chapter Summary	35
CHAPTER FOUR: STBC-DFE SCHEMES COMBINED WITH CONVOLUTIONAL CODES.....	36
4.1 Convolutional Codes.....	36
4.1.1 Convolutional Codes Generation	37
4.1.2 Hamming Distance in Convolutional Codes	38
4.2 Decoding of Convolutional Codes.....	38
4.3 STBC-DFE Combined with Convolutional Codes.....	43
4.4 Computer Simulations and Analysis.....	44
4.4.1 STBC-DFE Combined with Convolutional Codes for Multi-user Case One..	44

4.4.2 STBC-DFE Combined with Convolutional Codes for Multi-user Case Two	46
4.5 Chapter Summary	48
CHAPTER FIVE: PERFORMANCE COMPARISON BETWEEN STBC-OFDM AND STBC-DFE.....	49
5.1 Orthogonal Frequency Division Multiplexing Theory	51
5.2 Fast Fourier Transform for OFDM Modulation and Demodulation.....	52
5.3 STBC-OFDM System.....	56
5.4 Computer Simulations and Analysis.....	57
5.5 Chapter Summary	58
CHAPTER SIX: CONCLUSIONS.....	59
REFERENCES	61

LIST OF TABLES

Table 3.1 Channels between Transmit and Receive Antennas	21
Table 3.2 Encoding and Transmit Sequence.....	21
Table 3.3 Receive Signals at the Two Receive Antennas.....	21
Table 3.4 Outputs of STBC-DFE.....	25
Table 3.5 Typical Urban Channel Power Delay Profile	28

LIST OF FIGURES

Figure 1.1 Digital Communication System Diagram	1
Figure 2.1 FIR MIMO DFE Diagram.....	13
Figure 2.2 SISO-DFE BER Performance	15
Figure 3.1 Multi-transmit Multi-receive Antenna Space-Time Coding System.....	19
Figure 3.2 STBC Encoding Diagram.....	20
Figure 3.3 Block Diagram of STBC-DFE for the First Decoding Method	26
Figure 3.4 Block Diagram of STBC-DFE for the Second Decoding Method.....	27
Figure 3.5 Performance Comparison of STBC-DFE with Different Taps Using BPSK Modulation (Multi-user Case One).....	29
Figure 3.6 Performance Comparison of STBC-DFE with Different Decoding Methods Using BPSK Modulation (Multi-user Case One)	30
Figure 3.7 BER vs. SNR Performance Using the First Decoding Method (Multi-user Case One).....	31
Figure 3.8 Performance Comparison of STBC-DFE with Different Taps Using BPSK modulation (Multi-user Case Two).....	32
Figure 3.9 Performance Comparison of STBC-DFE with Different Decoding Methods Using BPSK Modulation (Multi-user Case Two).....	33
Figure 3.10 BER vs. SNR Performance Using the First Decoding Method (Multi-user Case Two)	34
Figure 4.1 General Encoder of Convolutional Codes.....	37
Figure 4.2 Trellis and Status Diagram.....	40
Figure 4.3 System Structure of STBC-DFE combined with Convolutional Codes (using the first decoding method)	43
Figure 4.4 System Structure of STBC-DFE combined with Convolutional Codes (using the second decoding method).....	44

Figure 4.5 Performance Comparison of the System Combining Convolutional Codes and STBC-DFE using Different Decoding Methods (Multi-user Case One).....	45
Figure 4.6 Performance Comparison of the STBC-DFE Systems with and without Convolutional Codes (Multi-user Case One).....	46
Figure 4.7 Performance Comparison of the System Combining Convolutional Codes and STBC-DFE using Different Decoding Methods (Multi-user Case Two)	47
Figure 5.1 OFDM Modulation/Demodulation.....	52
Figure 5.2 FDM Spectrum and OFDM Spectrum	53
Figure 5.3 OFDM Modulation Using IFFT	54
Figure 5.4 OFDM Modulation Using FFT	55
Figure 5.5 STBC-OFDM System	56
Figure 5.6 Performance Comparison among Three Systems Using the First Decoding Method	57

CHAPTER ONE: INTRODUCTION

In practical digital communication systems, the transmitted digital signals will experience errors inevitably due to non-ideal channel transmission and additive white Gaussian noise (AWGN). In order to achieve certain bit error rate with signal-noise-ratio known, proper design of base-band signals, selection of modulation/demodulation method, frequency/time domain equalization and time/space diversity are used to minimize bit error rate. Figure 1.1 is a typical digital communication system's structure (AWGN refers to additive Gaussian white noise in this figure).

Mobile radio channel is a time-variant fading channel with detrimental transmission situations due to the distortions from multi-path transmission and multi-path signal superposition. The antenna diversity technology can efficiently overcome these shortcomings, so it has gained a lot of attention. In general, antenna diversity technology uses multiple receive antennas to receive multi-path signals, then sum them up according to a certain rule.

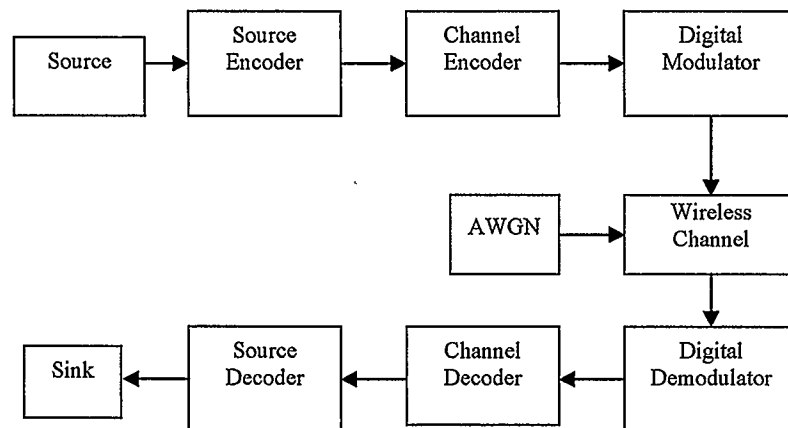


Figure 1.1 Digital Communication System Diagram

Normally, the communication system with multiple transmit antennas and multiple receive antennas is also called multi-input multi-output (MIMO) communication system. MIMO communication systems have been under extensive study, due to their ultra high spectrum efficiency. Essentially, MIMO communication systems use multiple transmitters to transmit multiple signals over the same carrier simultaneously so that large capacity increase is possible.

In MIMO systems, inter-symbol interference (ISI) results in distortions of transmitted signals, while equalization techniques help to recover the transmitted signals. Reduction of ISI is usually accomplished by use of pre-equalization at the transmitter and/or post-equalization at the receiver [1, 2]. At the transmitter, a compromise (or statistical) equalizer is usually designed to compensate for the average of the range of expected channel amplitude and delay characteristics. At the receiver, on the other hand, equalizers with adjustable coefficients are commonly used. The adjustment of the equalizer coefficients are performed by minimization of mean-square error (MSE) with the error defined as the difference between a known reference signal and its reconstructed version. The reference signal is called the training sequence, and it is sent by the transmitter at the start of the transmission. When the initial training period is completed, the coefficients of the adaptive equalizer may be continually adjusted in a decision-directed mode with the reconstructed sequence, obtained by applying the adaptive equalizer output to a decision device, serving as the reference. Normally equalization algorithms can be classified into two types: linear equalization (LE) and non-linear equalization (NLE). This thesis focuses on a particular nonlinear equalizer: decision feedback equalizer (DFE). Since DFE is first introduced by Austin in 1967, a great amount of attention has been paid to it

because of its advantages, such as improved performance over linear equalizers and reduced computation complexity compared to the other nonlinear equalizers. A decision feedback equalizer consists of a feed-forward filter that filters the received signals and a feedback filter which filters previously received symbols and cancels their impact on the output of the feed-forward filter. The feed-forward and feedback filtered signals are combined and fed into a decision device which makes decisions on a symbol by symbol or on a block of symbols basis.

Note that bit error rate can be further reduced by channel coding (or error control coding) to achieve the goal. Space-time coding technology, which has attracted extensive attention from researchers, is a new anti-interference technology, which is a combination of antenna diversity technology and error correction coding technology. It has very good anti-fading performance in mobile fading channels. One of the popular space-time coding methods is Space-Time Trellis Coding (STTC). It combines encoding, modulation, transmit diversity and arbitrary receive diversity, and has good performance, while the complexity and decoding time delay increase as well [3]. Space-Time Block Coding (STBC) can achieve maximum diversity $n_T \times n_R$ (n_T and n_R are the number of transmit and receive antennas, respectively) and minimize decoding time delay with simpler decoding algorithm compared with other algorithms. In this thesis, a combination of STBC and DFE using two new decoding methods is proposed. We call this combination STBC-DFE. Note that utilizing space-time codes' advantages is at the cost of increased system complexity, hence, comprehensive consideration of system complexity and performance is very important.

However, STBC can not achieve additional coding gain. It must be connected with some outer codes which have better coding gain to obtain improved performance. Coded modulation (CM) can efficiently improve transmission quality in communication system by the integrated optimization of encoding and modulation in Euclidean space. CM is first proposed by Massey in 1974 [4]. In 1982, Ungerboeck clearly formalized this idea in his milestone paper [5]. When convolutional codes are used, the coding method is called trellis-coded modulation (TCM). The definition and principles of TCM are presented in [6]. Recently, the study about TCM mainly focuses on applications in many areas, and more attention has been given to a fast developing communication system, i.e. mobile communication.

On the basis of mobile channel model, this thesis applies the combination of TCM and STBC-DFE to further improve the performance. Here convolutional codes are outer codes for STBC. The systems which utilize two new decoding methods, satisfy the requirements of the next generation of mobile communications. The proposed methods are reliable and not very complex.

In order to prove and compare the effectiveness of the proposed STBC-DFE methods with another advanced anti-ISI technology, orthogonal frequency division multiplexing (OFDM) is also introduced in this thesis. OFDM or multi-tone transmission is a special multi-carrier modulation and highly efficient data transmission method. OFDM consists in dividing the input symbol stream in several parallel streams which are used to modulate orthogonal carriers. As the carriers are orthogonal on the symbol duration, they do not interfere when the channel is of the additive white Gaussian noise type. On the other hand, because of the parallel transmission, the symbol duration is increased and the

system is more resistant to large delay spreads. It also has good resistance to narrowband interference and increases frequency spectrum efficiency greatly [7, 8]. This technique has been widely used for several applications [8-11]. These papers introduce the technique of guard interval which is very elegant to cope with a dispersive channel. This method also maps the linear convolution corresponding to the channel into a circular one. Hence, Discrete Fourier Transformation (DFT) may be used at the receiver. When multi-tone modulation is implemented by a digital device, it is often referred to as discrete multi-tone (DMT). Most of the attention has been devoted to multi-tone systems with guard time. In [11], Kalet has shown how it is possible to take advantage of the different sub-channels characteristics by varying the data rates and transmission powers among them. In [12], an OFDM system with optimized allocation of power and data among the sub-channels, was designed for asymmetric digital subscriber line (ADSL). The performance of an optimized multi-carrier system is investigated and compared to the performance achieved by means of an equalized single carrier (SC) transmission system in [13]. The authors of [13] claimed that for additive white Gaussian noise (AWGN) channels or near end cross talk (NEXT) channels, the multi-carrier (MC) system outperforms the single-carrier (SC) one with minimum-mean-square-error (MMSE) equalization. The combination of convolutional coding and STBC-DFE is compared with OFDM system in this thesis.

The structure of single-input single-output (SISO) DFE scheme is introduced and simulation results of this scheme are analyzed in chapter two. The structure of MIMO-DFE and the multiple-input multiple-output Rayleigh fading channel used in this thesis are also described in this chapter. The concatenation of Space-Time Block Coding

and DFE is narrated in details and the simulation results are analyzed in chapter three. The encoding and decoding of convolutional codes are introduced in chapter four. In the same chapter, the structure and simulation results of the scheme combining convolutional codes and STBC-DFE are given and analyzed. OFDM system theory is introduced in chapter five. The simulation results of the STBC-OFDM system with the same channel conditions are analyzed and compared with the simulation results of STBC-DFE system. Chapter six contains the conclusions of this thesis.

CHAPTER TWO: SISO-DFE SYSTEM AND MIMO-DFE SYSTEM

Multi-input multi-output (MIMO) communication systems have been under extensive study, because of their ultra high spectrum efficiency. In MIMO systems, inter-symbol interference (ISI) results in distortions of transmitted signals, while equalization techniques help to recover the transmitted signals. Normally, the equalization algorithms are classified into two parts [14, 15]: linear equalization and non-linear equalization. In this thesis, we focus on a nonlinear equalizer - Decision Feedback Equalizer (DFE). Since DFE is first introduced by Austin in 1967, a great amount of attention has been paid to it because of its advantages, such as improved performance over linear equalizers and reduced computation complexity compared to the other nonlinear equalizers. In the case of multi-path propagation, it is reasonable to expect that different signal paths impinge on the receiver antenna from different angles. It can be utilized to perform equalization in the spatial domain, i.e. we use an antenna array to separate different signal paths from each other. The decision-feedback equalizer (DFE) was established as a canonical receiver structure by Price in 1971 [16]. Salz[17], Messerchmitt[18], Belfiore and Park[19] studied various enhancements and restrictions for the DFE. Price first proposed that at high SNR the DFE could be combined with coding at the other modulation schemes. Zervos and Kalet [20] confirmed this proposal. They also studied zero-forcing DFE which requires very high SNR, which sometimes is impractical. Cioffi, Dudevoir, Eyuboglu, and Forney[21] extended the optimality result of the minimum-mean-square-error (MMSE) DFE for arbitrary SNR, and introduced the informative relation between the receiver SNR and the mutual information I of the channel according to [2]:

$$\text{SNR}_{\text{MMSE-DFE}}=2^I.$$

For an optimal transmitter, $I \rightarrow C$ where C is the water-pouring capacity of the channel. In order to establish this result, infinite length receive and transmit filters, with the optimum transmit filter synthesizing the “water-pouring” spectral shape necessary for capacity [22] were derived in [21]. Compared with the infinite-impulse-response DFE, the optimization of finite-impulse-response DFE receives more attention because it can be easily implemented in practice. In the case of multi-path propagation it is reasonable to expect that different signal paths impinge on the receiver antenna from different angles. This fact can be utilized to perform equalization in the spatial domain, i.e. we use an antenna array to separate different signal paths from each other. We can then use either only one of the signal paths, the strongest one, or we can use a combination of all the signal paths together. This is an example of spatial equalization. In this thesis we consider the case of combined spatial and temporal equalization by means of a combination of multiple transmit and receive antennas and a DFE equalization scheme.

Normally the coefficients of DFE are estimated by a certain estimation algorithm. With channel impulse response (CIR) parameters known, the maximum likelihood sequence estimation (MLSE), implemented by the Viterbi algorithm (VA) [23], can achieve an optimum performance, but the implementation complexity of the MLSE increases exponentially with M^L where L is the length of the overall channel impulse response and M is the number of modulation levels. Therefore, it is difficult to implement the MLSE for QPSK or higher modulations corrupted by severe selective multi-path fading. A lot of research has been undertaken to achieve the performance of the MLSE at reduced complexity [24]-[31]. Most of the early work concentrated on preprocessing techniques

to reduce the channel impulse response to a short length [24]-[28]. In [24] a linear equalizer was used to reduce the overall impulse response. In [25] and [26] the optimization of the desired impulse response for a fixed length was investigated. Lee [27] used a separate DFE with hard decision to truncate part of the postcursors. Cheung [28] used a separate DFE with soft decision feedback to reduce the channel impulse response, for ISI introduced by continuous phase modulation. Eyuboglu [29] proposed reduced-state sequence estimation (RSSE) with set partitioning and decision feedback, which is more applicable to high-level modulations. Duel-Hallen [30] proposed a delayed-decision feedback sequence estimator (DDFSE). Both RSSE and DDFSE assume the first sample of overall channel impulse response is unity and no precursors are considered. In [31], a reduced-complexity multi-channel DFE is proposed.

In the analysis of a DFE, usually it is assumed that the receiver has perfect knowledge of the channel impulse response. However, this is not the case in practice, and for a rapidly fading channel, errors in channel tracking can become significant. Due to its low computational complexity and near optimal performance, the DFE operating under a suitable adaptive algorithm, is used in a variety of time-dispersive fading channels, such as a mobile radio channel, a troposcatter channel, or an underwater acoustic channel. The critical issue for DFE's performance in a rapidly changing channel is the tracking capability of the underlying adaptive algorithm. The primary factor which causes the degradation of the DFE performance from the matched filter bound is the residual ISI from previous symbols. The impact of ISI on the average achievable bit error probability has been theoretically analyzed in [32], assuming that the channel state information is completely known.

When an incorrect decision is made by a DFE, the ISI cancellation becomes flawed for future decisions, a phenomenon known as error propagation. The error propagation will have a relatively minor effect on the detector's bit error rate. The reason is that the effect of incorrect feedback by the nonlinear decision device is usually short, so that continuous bursts of errors do not significantly degrade performance [33].

2.1 SISO-DFE System

For comparison with MIMO-DFE, the single-input single-output (SISO) DFE is first introduced. Assume a single-input single-output Rayleigh fading channel with additive white Gaussian noise (AWGN). Rayleigh fading is a statistical model for the effect of a propagation environment on a radio signal. It assumes that the power of a signal that has passed through a transmission medium (also called a communications channel) will vary randomly, or fade, according to a Rayleigh distribution (the radial component of the sum of two orthogonal variables which are independent and normally distributed with unit variance). AWGN is the noise having a frequency spectrum that is continuous and uniform over a specified frequency band. The channel memory is L . The channel output at time k is given by

$$y_k = \sum_{m=0}^L h_m x_{k-m} + n_k \quad (2.1)$$

where h_m is channel coefficient and n_k is additive white Gaussian noise.

In the DFE, the feedforward filter has $N+1$ taps; the feedback filter has M taps. At time k , the coefficients of the feedforward filter and the feedback filter are a_i ($i=0,1,\dots,N$) and b_j ($j=1,2,\dots,M$), respectively. And the coefficient vectors are denoted as

$\mathbf{a}_k = [a_0, a_1, \dots, a_N]^T$ and $\mathbf{b}_k = [b_1, b_2, \dots, b_M]^T$. For a block of $L+1$ outputs from the DFE, the formula (2.2) could be derived.

$$\begin{bmatrix} z_k^* \\ z_{k-1}^* \\ \vdots \\ z_{k-L+1}^* \end{bmatrix} = \begin{bmatrix} \mathbf{y}_k^* & \hat{\mathbf{x}}_{k-1}^* \\ \mathbf{y}_{k-1}^* & \hat{\mathbf{x}}_{k-2}^* \\ \vdots & \vdots \\ \mathbf{y}_{k-L+1}^* & \hat{\mathbf{x}}_{k-L}^* \end{bmatrix} \begin{bmatrix} \mathbf{a}_k \\ \mathbf{b}_k \end{bmatrix} + \begin{bmatrix} \mathbf{e}_k \\ \mathbf{e}_{k-1} \\ \vdots \\ \mathbf{e}_{k-L+1} \end{bmatrix} \quad (2.2)$$

$$\mathbf{y}_k^* = [y_{k-N+1}^* \quad y_{k-N+2}^* \quad \cdots \quad y_{k-1}^* \quad y_k^*] \quad (2.3)$$

$$\hat{\mathbf{x}}_{k-1}^* = [x_{k-1}^* \quad x_{k-2}^* \quad \cdots \quad x_{k-M+1}^* \quad x_{k-M}^*] \quad (2.4)$$

where $(\cdot)^*$ denotes the complex conjugate transpose operation. (2.2) also can be written in matrix form

$$\bar{\mathbf{z}}_{k,L} = \mathbf{D}_{k,L} \mathbf{c}_k + \mathbf{e}_{k,L} \quad (2.5)$$

where $\mathbf{c}_k = [a_0, a_1, \dots, a_N, b_1, b_2, \dots, b_M]^T$ and each row in $\mathbf{D}_{k,L}$ is denoted as \mathbf{d}_j^* .

When the DFE is in training, the DFE output z_k is assumed same with the channel input x_k . In practice, this assumption is valid most of the time due to high signal-to-noise operation conditions and the training sequences. The block iterative normalized least-mean-squares (BINLMS) algorithm proposed in [34], is used in the DFE training.

The BINLMS update formula is

$$\begin{aligned} \hat{\mathbf{c}}_{k,i+1} &= \hat{\mathbf{c}}_{k,i} + \mu \varepsilon_i^* \frac{\mathbf{d}_j}{\mathbf{d}_j^* \mathbf{d}_j} \\ \varepsilon_i &= \hat{x}_j - \hat{\mathbf{c}}_{k,i} \mathbf{d}_j \end{aligned} \quad (2.6)$$

where i ($i=1,2,\dots,L,\dots,KL$) is the iteration index, K indicates the system's maximum allowable processing load, j ($j=k-(i \bmod L)$) is the equation index, k ($k=L,2L,3L,\dots$) is the time index, and $0 < \mu < 2$ is the step size.

2.2 Multiple-Input Multiple-Output Rayleigh Fading Channel

To provide exactly specified, identical test conditions, implementations of different receivers are evaluated. In particular the equalizers, a set of typical channel impulse responses are defined in GSM standard [35]. Here we use one of the models: Typical Urban model. The channel distribution is Rayleigh fading.

Consider a two-input two-output Rayleigh fading channel with additive white Gaussian noise (AWGN). The channel memory is v . The received signals $y_k^{(1)}$ and $y_k^{(2)}$ at time k are given by

$$\mathbf{y}_k = \begin{bmatrix} y_k^{(1)} \\ y_k^{(2)} \end{bmatrix} = \sum_{m=0}^v \mathbf{H}_m \mathbf{x}_{k-m} + \mathbf{n}_k \quad (2.7)$$

where \mathbf{H}_m is the m th channel coefficients matrix of size 2 by 2, \mathbf{n}_k is additive white Gaussian noise.

For a block of N_f received symbols, we have

$$\begin{bmatrix} \mathbf{y}_{k+N_f-1} \\ \mathbf{y}_{k+N_f-2} \\ \vdots \\ \mathbf{y}_k \end{bmatrix} = \begin{bmatrix} \mathbf{H}_0 & \mathbf{H}_1 & \cdots & \mathbf{H}_v & 0 & \cdots & 0 \\ 0 & \mathbf{H}_0 & \mathbf{H}_1 & \cdots & \mathbf{H}_v & 0 & \cdots \\ \vdots & & \ddots & & \ddots & & \\ 0 & \cdots & 0 & \mathbf{H}_0 & \mathbf{H}_1 & \cdots & \mathbf{H}_v \end{bmatrix} \begin{bmatrix} \mathbf{x}_{k+N_f-1} \\ \mathbf{x}_{k+N_f-2} \\ \vdots \\ \mathbf{x}_{k-v} \end{bmatrix} + \begin{bmatrix} \mathbf{n}_{k+N_f-1} \\ \mathbf{n}_{k+N_f-2} \\ \vdots \\ \mathbf{n}_k \end{bmatrix} \quad (2.8)$$

2.3 MIMO-DFE System

By using training sequence, we can obtain estimates of the channel matrix [36]. Here we assume the estimates are perfect. We adopt minimum-mean-square-error method to

compute the optimal coefficients of finite impulse response (FIR) decision feedback equalizer (DFE) according to the channel estimates. The structure of the two-input two-output FIR DFE is shown in Figure 2.1. Some definitions are given as follows:

Input auto-correlation matrix:

$$\mathbf{R}_{xx} = E[\mathbf{x}_{k+N_f-1:k-v} \mathbf{x}_{k+N_f-1:k-v}^*] \quad (2.9)$$

Noise auto-correlation matrix:

$$\mathbf{R}_{nn} = E[\mathbf{n}_{k+N_f-1:k} \mathbf{n}_{k+N_f-1:k}^*] \quad (2.10)$$

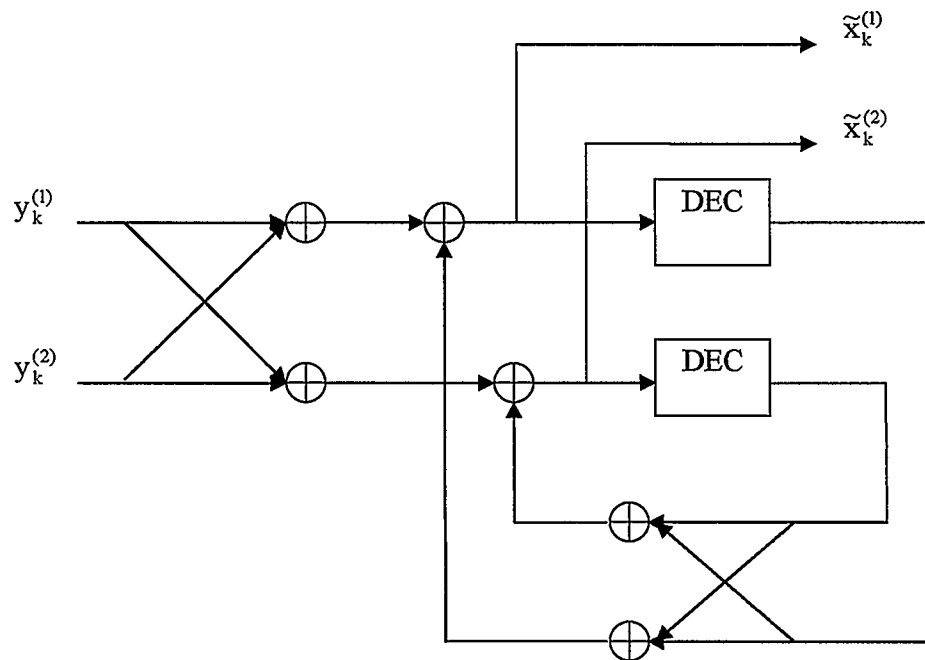


Figure 2.1 FIR MIMO DFE Diagram

Output auto-correlation matrix:

$$\mathbf{R}_{yy} = E[\mathbf{y}_{k+N_f-1:k} \mathbf{y}_{k+N_f-1:k}^*] = \mathbf{H} \mathbf{R}_{xx} \mathbf{H}^* + \mathbf{R}_{nn} \quad (2.11)$$

In the FIR MMSE-DFE, the feed-forward filter matrix is

$$\mathbf{W}^* = [\mathbf{W}_0^* \quad \mathbf{W}_1^* \quad \cdots \quad \mathbf{W}_{N_f-1}^*] \quad (2.12)$$

where \mathbf{W}_0^* is of size $n_0 \times n_i$ (n_0 and n_i are the number of output and input of DFE respectively); N_f is the number of feedforward filter taps in DFE; the feedback filter matrix is

$$[\mathbf{I}_{n_i} \quad \mathbf{0}_{n_i \times n_b}] - \mathbf{B}^* = [(\mathbf{I}_{n_i} - \mathbf{B}_0^*) \quad -\mathbf{B}_1^* \quad \cdots \quad -\mathbf{B}_{N_b}^*] \quad (2.13)$$

where $\mathbf{B}^* = [\mathbf{B}_0^* \quad \mathbf{B}_1^* \quad \cdots \quad \mathbf{B}_{N_b}^*]$ (N_b is the number of feedback filter taps in DFE) and \mathbf{B}_i is of size $n_i \times n_i$. With definition $\tilde{\mathbf{B}}^* = [\mathbf{0}_{n_i \times n_i \Delta} \quad \mathbf{B}^*]$, the MIMO MMSE-DFE error vector at time k is

$$\mathbf{E}_k = \tilde{\mathbf{B}}^* \mathbf{x}_{k+N_f-1:k-v} - \mathbf{W}^* \mathbf{y}_{k+N_f-1:k} \quad (2.14)$$

Then the error auto-correlation matrix:

$$\mathbf{R}_{ee} = E[\mathbf{E}_k \mathbf{E}_k^*] \quad (2.15)$$

In order to get the optimal coefficients of DFE, we solve the following optimization problem:

$$\min_{\tilde{\mathbf{B}}} \text{trace}(\mathbf{R}_{ee}) = \min_{\tilde{\mathbf{B}}} \text{trace}(\tilde{\mathbf{B}}^* \mathbf{R}^{-1} \tilde{\mathbf{B}}) \quad (2.16)$$

In the next chapter, the solution to the above optimization problem will be given.

2.4 Computer Simulations and Analysis

We consider the SISO Rayleigh fading channel with memory $L=3$, the feedback filter in SISO-DFE has 3 taps. The step size of block iterative normalized least mean squares algorithm (BINLMS) is 0.008. Figure 2.2 shows BER vs. SNR performance when the SISO-DFE feedforward filter (FF) taps change. In Figure 2.2, it is evident that when the FF taps increase from 4 to 20, the performance gets a lot better, but the result is still not satisfactory. Some experiments were also done with FF taps equal to 30 and higher, the system performance is not any better. Hence, DFE using BINLMS is not effective in a SISO system. The similar conclusion can be mathematically deduced for a MIMO system.

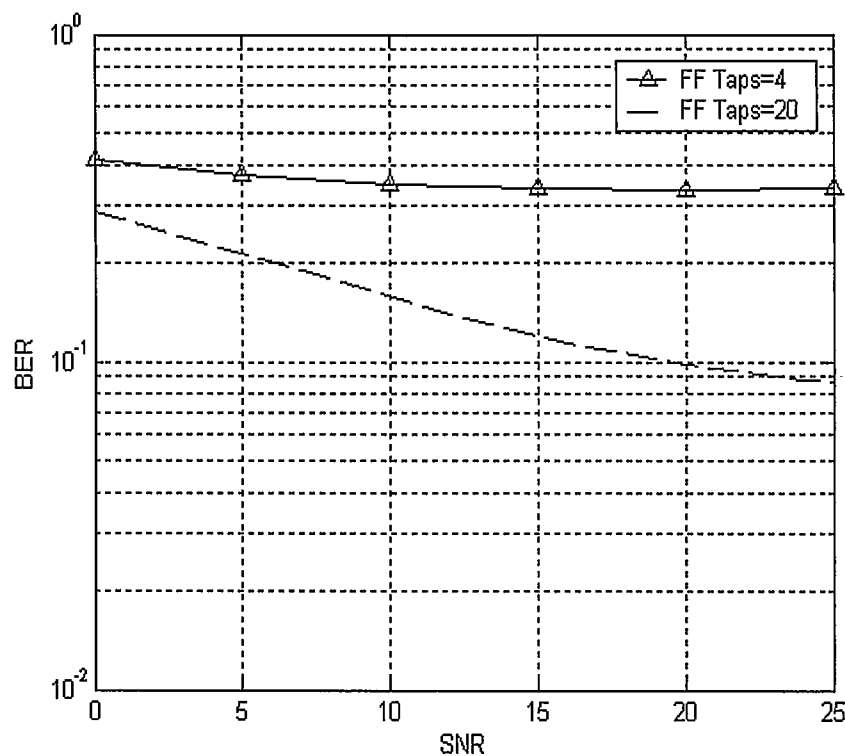


Figure 2.2 SISO-DFE BER Performance

2.5 Chapter Summary

In this chapter, the structure of SISO-DFE is described. BINLMS adaptive algorithm is used to optimize the coefficients of the SISO-DFE in the computer simulations. The simulation results show that DFE using BINLMS can't get good results in a SISO system. The MIMO Rayleigh fading channel is described and the structure of MIMO-DFE is also given. In the next chapter, we focus on a MIMO-DFE detection scheme where the estimation of the coefficients of the MIMO-DFE is perfect.

CHAPTER THREE: CONCATENATION OF SPACE-TIME BLOCK CODING AND DECISION FEEDBACK EQUALIZER

As information industry develops at a very high speed, there is a higher demand for effective and reliable high data rate transmission, especially in the third generation wireless multimedia wideband transmission. In the current information theory research, one of the critical problems is to minimize the transmission bit error rate without expanding signal frequency band and decreasing data rate. Also due to multi-path transmission and the superposition of multi-path signals, wireless channels are time variant fading channels with detrimental conditions. Antenna diversity can solve these problems, so it has attracted extensive attention. In general, antenna diversity technology uses multiple receive antennas to receive multi-path signals and sum up the received signals according to certain rules.

In practical communications systems, with signal-noise-ratio (SNR) known, channel codes, frequency equalization and modulation are used to meet system requirements. However, band-limited high data rate transmission is very difficult to be realized if only one error control technology is used. The space-time codes proposed by Calderbank and Tarokh [3], are a good solution to this problem. Space-time coding technology is a combination of channel coding and antenna diversity technology. It is also a new error correction coding and anti-error technology. It has good anti-error performance in wireless channels. With high reliability and high data rate, it efficiently utilizes the potential channel capacity in partitioning technology. Hence, it is very suitable for wireless multimedia communications and gains extensive study.

There are two popular space-time coding methods: Space-Time Trellis Coding (STTC) and Space-Time Block Coding (STBC). Combining error correction coding, modulation, diversity transmission and optional diversity reception, STTC achieve considerable performance gains. However, STTC increase processing complexity and decoding delay. For some applications, it is not practical or cost-effective. With simpler coding algorithm and minimum coding delay, STBC can achieve maximum spatial diversity $n_t \cdot n_r$, where n_t and n_r are the number of transmit antennas and receive antennas respectively. The STBC scheme has small computation complexity and does not require any feedback from the receiver to the transmitter [38]. While STBC can not achieve additional coding gain, it must be connected with some outer codes which have better coding gain to get improved performance. In the following content of this chapter, the space-time block coding will be introduced in detail.

3.1 Encoding and Decoding of Space-Time Coding

Multiple transmit and multiple receive antennas are used in space-time coding. In space-time coded multiple antennas systems, the binary sequence coded from original data by some proper coding algorithm, are divided into n sub-sequences and transmitted from n transmit antennas. Each receive antenna receives a signal sequence which is the summation of n transmitted sequences interfered by noise. The structure of space-time codes utilizing multiple transmit and multiple receive antennas, is shown in Figure 3.1.

In this figure, spatial diversity modulator transforms the coded binary sequence from serial to parallel, then delays and modulates it. Spatial diversity modulator and channel code encoder compose the space-time codes encoder. The received signals are demodulated in spatial diversity demodulator and decoded in space-time decoder serially.

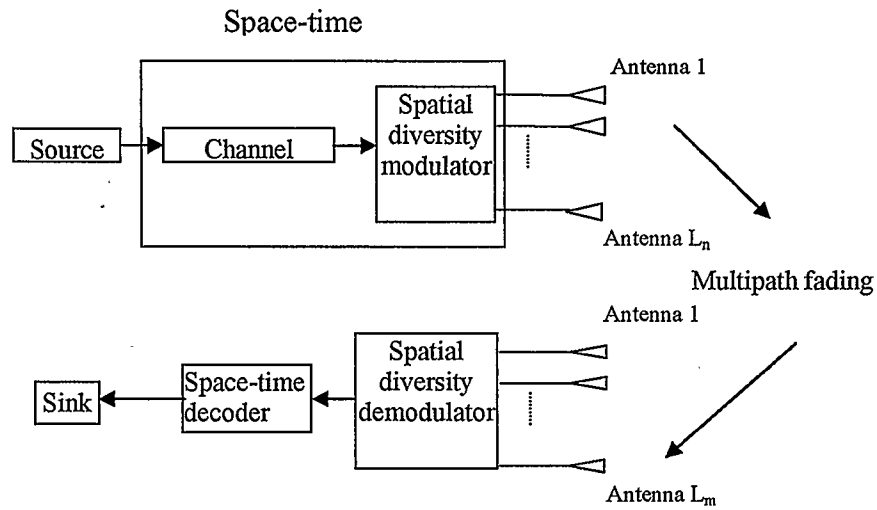


Figure 3.1 Multi-transmit Multi-receive Antenna Space-Time Coding System

Viterbi Maximum Likelihood decoding can be used in space-time decoder. Note that according to different space-time encoding algorithms, the structures of spatial diversity modulator and demodulator are varied.

3.2 Space-Time Block Coding

Space-Time Block Coding (STBC) proposed by Alamouti [38], uses two transmit antennas. The decoding complexity of STBC is much lower than that of STTC with two antennas and its performance is worse. Figure 3.2 shows the structure of STBC encoder. The encoder input is a complex signal sequence $x_i, i=1, \dots, K$ from some multi-tone modulation constellation. In the encoder, this input is mapped to the elements of matrix G with dimension $p \times n_T$, where n_T is the number of transmit antennas. The elements in matrix G include K complex signals x_i , their conjugate complex signals x_i^* and the

linear combination of x_i and x_i^* . Matrix G is a complex wide-sense orthogonal matrix, whose columns are orthogonal to each other [2, 38]. For example, $n_T=2$:

$$G = \begin{bmatrix} g_{11} & \cdots & g_{1n_T} \\ \vdots & & \vdots \\ g_{p1} & \cdots & g_{pn_T} \end{bmatrix} = \begin{bmatrix} x_1 & x_2 \\ -x_2^* & x_1^* \end{bmatrix} \quad (3.1)$$

the n_T elements of a row in matrix G are sent by n_T different antennas synchronously; all the elements of a column are sent by one identical antenna at p continuous transmit durations. There are n_R receive antennas in the receiver. Take $n_T = n_R = 2$ as an example, the decoding of STBC is as follows. The channels between the transmit and receive antennas are defined in Table 3.1, and the notations of the transmission sequence and the receive signals are given in Table 3.2 and Table 3.3.

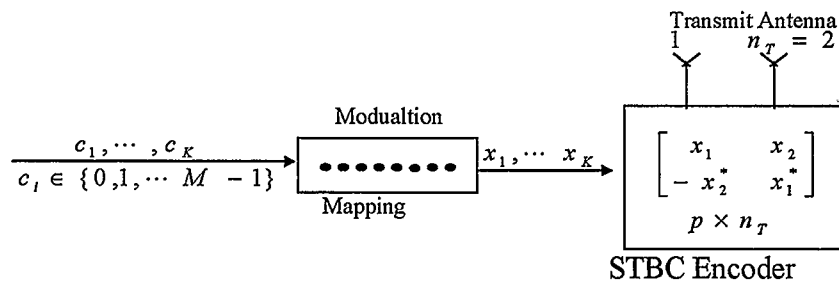


Figure 3.2 STBC Encoding Diagram

Table 3.1 Channels between Transmit and Receive Antennas

	rx antenna 0	rx antenna 1
tx antenna 0	h_0	h_2
tx antenna 1	h_1	h_3

Table 3.2 Encoding and Transmit Sequence

	antenna 0	antenna 1
time k	s_0	s_1
time $k+1$	$-s_1^*$	s_0^*

Table 3.3 Receive Signals at the Two Receive Antennas

	rx antenna 0	rx antenna 1
time k	r_0	r_2
time $k+1$	r_1	r_3

From the above tables, the following relations between the transmission sequence and the receive signals can be obtained.

$$\begin{aligned}
r_0 &= h_0 s_0 + h_1 s_1 + n_0 \\
r_1 &= -h_0 s_1^* + h_1 s_0^* + n_1 \\
r_2 &= h_2 s_0 + h_3 s_1 + n_2 \\
r_3 &= -h_2 s_1^* + h_3 s_0^* + n_3
\end{aligned} \tag{3.2}$$

where n_0 , n_1 , n_2 and n_3 are complex random variables representing receiver thermal noise and interference. The decoding formulas are as following,

$$\begin{aligned}
\tilde{s}_0 &= h_0^* r_0 + h_1 r_1^* + h_2^* r_2 + h_3 r_3^* \\
\tilde{s}_1 &= h_1^* r_0 - h_0 r_1^* + h_3^* r_2 - h_2 r_3^*
\end{aligned} \tag{3.3}$$

Note that the combined signals from the two receive antennas are the simple addition of the combined signals from each antenna. This principle can be easily generalized to the system with two transmit and M receive antennas. That is to say $2M$ diversity order can be gained by the simple addition of the combined signals from all the receive antennas.

3.3 Other Space-Time Codes

Generally for the space-time coding, there is an assumption that the channel fading factor is known in the receiver. But when the channel fading is serious and data rate is very high, it's not easy for the receiver to obtain the channel fading factor. In fact, to achieve high data rate and low bit error rate, the number of transmit antennas is larger, which makes the training time much longer and correspondingly this reduces the effective information transmission time. Especially for fast fading situation, it's not possible for receiver to get even few channels' fading factors. The Unitary Space-Time Modulation proposed in [39] is a space-time codes design for the situation that the fading factor is unknown in the receiver. This algorithm is almost optimal when SNR is very high. Hence, it is very suitable to fast Rayleigh fading channels.

The paper [39] presents a research direction for space-time coding: for various channels, various space-time codes should be explored. It has directive theoretic significance in the applications of space-time coding.

3.4 STBC-DFE Scheme Structure

3.4.1 DFE for Multi-user Case One

Based on the MIMO Rayleigh fading channel and FIR MIMO-DFE described in chapter two, we assume that for the current user, the interfering effect of other users can be

suppressed. In order to get the optimal coefficients of DFE, we solve the optimization problem mentioned in (2.16). For convenience, we rewrite (2.16) as follows

$$\min_{\tilde{\mathbf{B}}} \text{trace}(\mathbf{R}_{ee}) = \min_{\tilde{\mathbf{B}}} \text{trace}(\tilde{\mathbf{B}}^* \mathbf{R}^{-1} \tilde{\mathbf{B}}) \quad (3.4)$$

\mathbf{R} is partitioned as $\mathbf{R} = \begin{bmatrix} \mathbf{R}_{11} & \mathbf{R}_{12} \\ \mathbf{R}_{12}^* & \mathbf{R}_{22} \end{bmatrix}$ where \mathbf{R}_{11} is of size $n_i(\Delta + 1) \times n_i(\Delta + 1)$. Then

$$\tilde{\mathbf{B}}_{\text{opt}} = \begin{bmatrix} \mathbf{R}_{11} \\ \mathbf{R}_{12}^* \end{bmatrix} \mathbf{R}_{11}^{-1} \mathbf{C} \quad (3.5)$$

$$\mathbf{R}_{ee, \text{min}} = \mathbf{C}^* \mathbf{R}_{11}^{-1} \mathbf{C} \quad (3.6)$$

where $\mathbf{C} = [\mathbf{0}_{n_i \times n_i \Delta} \quad \mathbf{I}_{n_i}]$ and Δ is the filter delay which is chosen to minimize the trace of $\mathbf{R}_{ee, \text{min}}$. Then the optimum feedforward filter matrix is

$$\mathbf{W}_{\text{opt}}^* = \tilde{\mathbf{B}}_{\text{opt}}^* \mathbf{H}^* (\mathbf{H} \mathbf{H}^* + \sigma_n^2 \mathbf{I}_{2N_f})^{-1} \quad (3.7)$$

The output of the feedforward filter is

$$\mathbf{r}_k = \begin{bmatrix} \mathbf{r}_k^{(1)} \\ \mathbf{r}_k^{(2)} \end{bmatrix} = \mathbf{W}_{\text{opt}}^* \mathbf{y}_{k+N_f-1:k} \approx \sum_{i=0}^{N_b} \mathbf{B}_{\text{opt},i}^* \mathbf{x}_{k-i} + \tilde{\mathbf{n}}_k \quad (3.8)$$

Assuming $\hat{\mathbf{x}}_{k-i} = \mathbf{x}_{k-i}$, the output of the feedback filter is

$$\mathbf{z}_k = \begin{bmatrix} \mathbf{z}_k^{(1)} \\ \mathbf{z}_k^{(2)} \end{bmatrix} = \mathbf{r}_k - \sum_{i=0}^{N_b} \mathbf{B}_{\text{opt},i}^* \hat{\mathbf{x}}_{k-i} \approx \mathbf{B}_{\text{opt},0}^* \hat{\mathbf{x}}_k + \tilde{\mathbf{n}}_k \quad (3.9)$$

In the above equation, the noise vector is correlated. The spatial correlation matrix of noise vector is

$$\mathbf{R}_{\tilde{\mathbf{n}}\tilde{\mathbf{n}}} = E[\tilde{\mathbf{n}}_k \tilde{\mathbf{n}}_k^*] = \sigma_n^2 \mathbf{W}_{\text{opt}}^* \mathbf{W}_{\text{opt}} \quad (3.10)$$

In [37], to preserve the simple decoding rule of STBC without performance loss, they did noise decorrelation as follows

$$\mathbf{R}_{\bar{\mathbf{n}}\bar{\mathbf{n}}} = \mathbf{U}\mathbf{\Gamma}\mathbf{U}^* \quad (3.11)$$

where \mathbf{U} is an orthogonal matrix of the eigenvectors of $\mathbf{R}_{\bar{\mathbf{n}}\bar{\mathbf{n}}}$ and $\mathbf{\Gamma}$ is a diagonal matrix of the eigenvalues of $\mathbf{R}_{\bar{\mathbf{n}}\bar{\mathbf{n}}}$. Hence, the coefficients and outputs of the MMSE-DFE have been replaced as:

$$\begin{aligned} \bar{\mathbf{W}}_{\text{opt}}^* &= \mathbf{U}^* \mathbf{W}_{\text{opt}}^* \quad \text{and} \quad \bar{\mathbf{B}}_{\text{opt}}^* = \mathbf{U}^* \mathbf{B}_{\text{opt}}^* \\ \bar{\mathbf{r}}_k &= \bar{\mathbf{W}}_{\text{opt}}^* \mathbf{y}_{k+N_f-1:k} \approx \sum_{i=0}^{N_b} \bar{\mathbf{B}}_{\text{opt},i}^* \hat{\mathbf{x}}_{k-i} + \bar{\mathbf{n}}_k \end{aligned} \quad (3.12)$$

$$\bar{\mathbf{z}}_k = \bar{\mathbf{r}}_k - \sum_{i=0}^{N_b} \bar{\mathbf{B}}_{\text{opt},i}^* \hat{\mathbf{x}}_{k-i} \approx \bar{\mathbf{B}}_{\text{opt},0}^* \hat{\mathbf{x}}_k + \bar{\mathbf{n}}_k \quad (3.13)$$

3.4.2 DFE for Multi-user Case Two

Here we assume that the lower indexed users are detected first and higher indexed users use the current decisions from lower indexed users in making their own decisions. That is to say \mathbf{B}_0 is a monic lower triangular matrix. The results in equations (3.5) and (3.6) can still be used in this case. The only change is now $\mathbf{C} = [\mathbf{0}_{n_i \times n_i \Delta} \quad \mathbf{B}_0^*]$, where \mathbf{B}_0 is an $n_i \times n_i$ monic lower triangular matrix. The \mathbf{R}_{11}^{-1} can be partitioned as follows

$$\mathbf{R}_{11}^{-1} = \begin{bmatrix} \mathbf{R}_1 & \mathbf{R}_2 \\ \mathbf{R}_2^* & \mathbf{R}_3 \end{bmatrix} \quad (3.14)$$

where \mathbf{R}_1 is $n_i \Delta \times n_i \Delta$, and \mathbf{R}_3 is $n_i \times n_i$. Hence, (2.12) can be simplified to

$$\mathbf{R}_{\text{ee,min}} = \mathbf{B}_0^* \mathbf{R}_3 \mathbf{B}_0 \quad (3.15)$$

The remaining part of multiple-user DFE is same with that of single user DFE.

3.4.3 Structure of STBC-DFE

It is well known that STBC works on two consecutive symbols. The FIR MIMO MMSE-DFE we presented is also based on symbol. That is to say that only when the interference due to $x_{k-i}^{(1)}$ (for $0 \leq i \leq N_b - 1$ and $j=1,2$) is cancelled, can the equalizer output at time $k+1$ be computed. Hence, before STBC decoding, tentative decisions are needed. In [40] three additional steps are proposed before STBC decoding.

- a) Compute tentative decisions on $x_k^{(i)}$ from $z_k^{(i)}$ only using ML rule

$$\hat{\mathbf{X}}_k = \begin{bmatrix} \hat{x}_k^{(1)} \\ \hat{\mathbf{X}}_k \\ \hat{x}_k^{(2)} \\ \hat{\mathbf{X}}_k \end{bmatrix} = \arg \min_{\hat{\mathbf{X}}_k} \left| \mathbf{z}_k - \overline{\mathbf{B}}_{\text{opt}}^* \hat{\mathbf{X}}_k \right|^2 = \arg \min_{\substack{\hat{x}_k^{(1)}, \hat{x}_k^{(2)} \\ \hat{\mathbf{X}}_k}} \sum_{i=1}^2 \sum_{j=1}^2 \left| z_k^{(i)} - \overline{\mathbf{B}}_{\text{opt},0}^*(i,j) \hat{x}_k^{(j)} \right|^2 \quad (3.16)$$

where $\overline{\mathbf{B}}_{\text{opt},0}^*(i,j)$ is the element located in the i th row and j th column of matrix $\overline{\mathbf{B}}_{\text{opt},0}^*$.

- b) Compute the outputs $z_{k+1}^{(i)}$ by using the FIR MIMO MMSE-DFE structure.
- c) STBC decoding by using the DFE outputs $z_k^{(i)}$ and $z_{k+1}^{(i)}$. All of the parameters are explained in Tables 3.1, 3.2 and 3.4.

Table 3.4 Outputs of STBC-DFE

	rx antenna 0	rx antenna 1
time k	$z_k^{(1)}$	$z_k^{(2)}$
time k+1	$z_{k+1}^{(1)}$	$z_{k+1}^{(2)}$

Based on the above three steps, two decoding methods will be introduced as follows:

- (1) Due to the ISI distortions in transmitted signals, the standard STBC decoding procedure (see formula (3.3)) can not be used for this STBC-DFE system directly.

According to the DFE, the standard STBC decoding can be changed as follows:

$$\begin{aligned}\tilde{s}_0 &= h_0^* z_k^{(1)} + h_1 z_{k+1}^{(1)*} + h_2^* z_k^{(2)} + h_3 z_{k+1}^{(2)*} \\ \tilde{s}_1 &= h_1^* z_k^{(1)} - h_0 z_{k+1}^{(1)*} + h_3^* z_k^{(2)} - h_2 z_{k+1}^{(2)*}\end{aligned}\quad (3.17)$$

where \tilde{s}_0 and \tilde{s}_1 are decoded signals, h_0 to h_3 are channel parameters and $z_k^{(j)}$ and $z_{k+1}^{(j)}$ ($j=1,2$) are outputs of the DFE at time k and $k+1$.

However, we can use the feedback filter matrix of DFE to replace the channel parameters in (3.17), so (3.17) can be rewritten as follows:

$$\begin{aligned}\tilde{s}_0 &= \mathbf{B}_0^*(1,1)z_k^{(1)} + \mathbf{B}_0(1,2)z_{k+1}^{(1)*} + \mathbf{B}_0^*(2,1)z_k^{(2)} + \mathbf{B}_0(2,2)z_{k+1}^{(2)*} \\ \tilde{s}_1 &= \mathbf{B}_0^*(1,2)z_k^{(1)} - \mathbf{B}_0(1,1)z_{k+1}^{(1)*} + \mathbf{B}_0^*(2,2)z_k^{(2)} - \mathbf{B}_0(2,1)z_{k+1}^{(2)*}\end{aligned}\quad (3.18)$$

The system structure of STBC-DFE of this method is shown in Figure 3.3. This diagram is similar to the system structure in [40], but we use formula (3.18) for the STBC decoder.

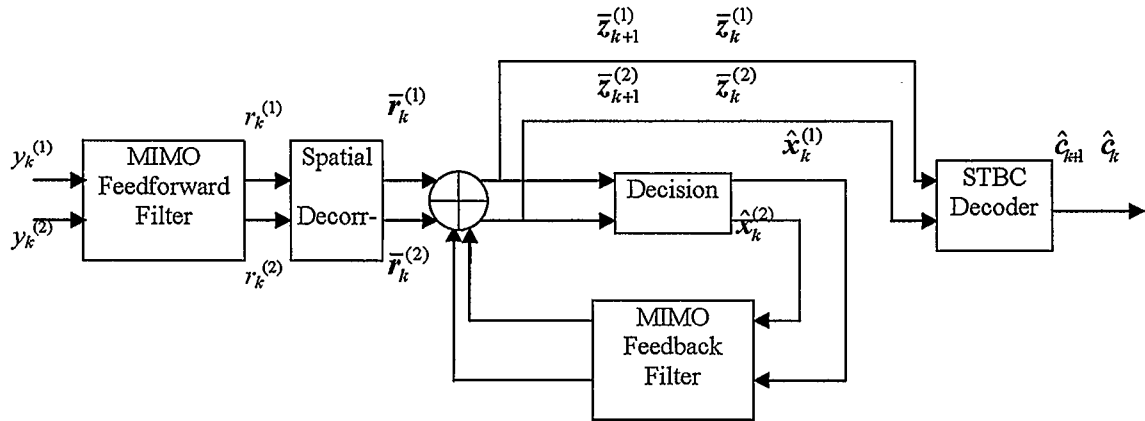


Figure3.3 Block Diagram of STBC-DFE for the First Decoding Method

(2) Also, there is an alternative method for the decoding of STBC-DFE. Considering the DFE has cancelled most of the detrimental effects caused by the channel, we can simplify formula (3.18) to:

$$\begin{aligned}\tilde{s}_0 &= z_k^{(1)} + z_{k+1}^{(1)*} + z_k^{(2)} + z_{k+1}^{(2)*} \\ \tilde{s}_1 &= z_k^{(1)} - z_{k+1}^{(1)*} + z_k^{(2)} - z_{k+1}^{(2)*}\end{aligned}\quad (3.19)$$

For the first method, the noise decorrelation is used to preserve the simple decoding rule of STBC without performance loss. However, this process also introduces the correlation to the DFE outputs. Hence, for the second system structure of STBC-DFE, we use formula (3.19) for the STBC decoder without the noise decorrelation part in the first method. The system structure with the second method is simplified consequently (see Figure 3.4).

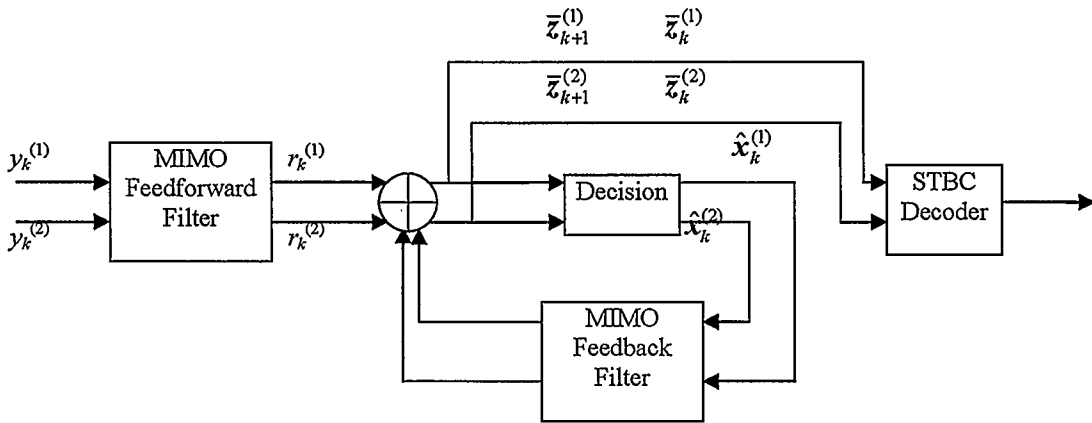


Figure 3.4 Block Diagram of STBC-DFE for the Second Decoding Method

3.5 Computer Simulations and Analysis

We simulated performances of the STBC-DFE systems with the two decoding methods for two multiple-user cases in Typical Urban channel where the channel memory equals three. Two transmit antennas and two receive antennas are used and each antenna transmits at half the transmit power of the single transmit antenna case. The number of feedback filter taps is 3, which is equal to the channel memory. The one bit interval is about 0.2 μ s. M-PSK modulation is used. The "PSK" refers to the use of phased shift keying which is a form of phase modulation accomplished by the use of a discrete number of states. Here, BPSK and 8PSK are used. They are PSK with 2 and 8 states respectively. The power delay profile of the channels is shown in Table 3.5. The channel power is normalized in the simulations.

Table 3.5 Typical Urban Channel Power Delay Profile

Delay(μ s)	0.0	0.2	0.5	1.6
Strength(dB)	-3.0	0.0	-2.0	-6.0

3.5.1 STBC-DFE for Multi-User Case One

(1) BPSK Modulation

For the multi-user case one, we assume that only previous estimates of the other users are known for each user, so it is equivalent to the single-user condition.

First, we compare the performances of the STBC-DFE systems with different feedforward filter taps (from 4 to 8). The decoding method for the STBC-DFE scheme is the first method. In Figure 3.5, for low SNR region (0 to 10 dB), when the number of feedforward filter taps (N_f) increases from 6 to 8, the performance improvement of the

STBC-DFE scheme is limited; for high SNR region, the BER performances are very different among the STBC-DFE schemes with various feedforward filter taps, i.e. the BER performance of STBC-DFE is much better as the number of feedforward filter taps increases.

Second, we compare the performances of the STBC-DFE schemes with the two decoding methods for STBC that we presented. The number of feedforward filter taps is fixed at 8 for these schemes. Figure 3.6 shows the simulation results of STBC-DFE with two decoding methods of STBC. In this figure, the first method has much better performance than the second method.

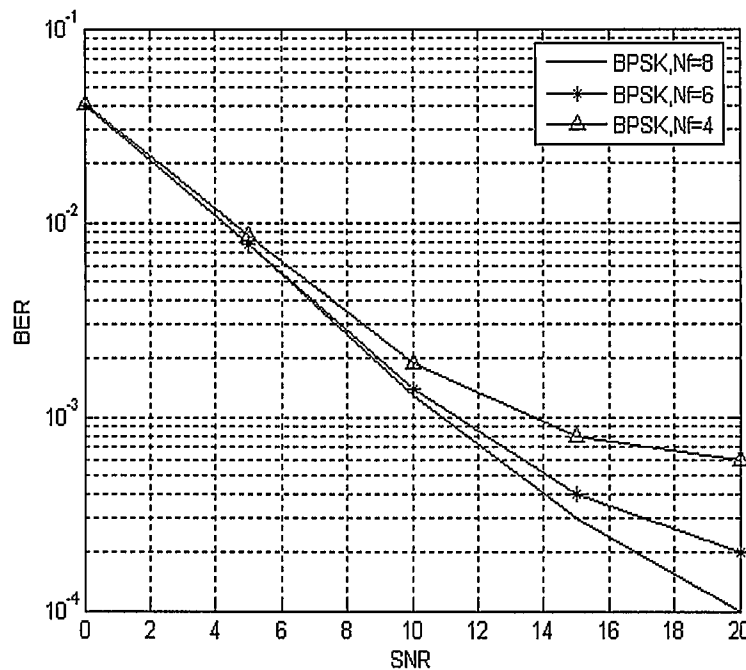


Figure 3.5 Performance Comparison of STBC-DFE with Different Taps Using BPSK Modulation(Multi-user Case One)

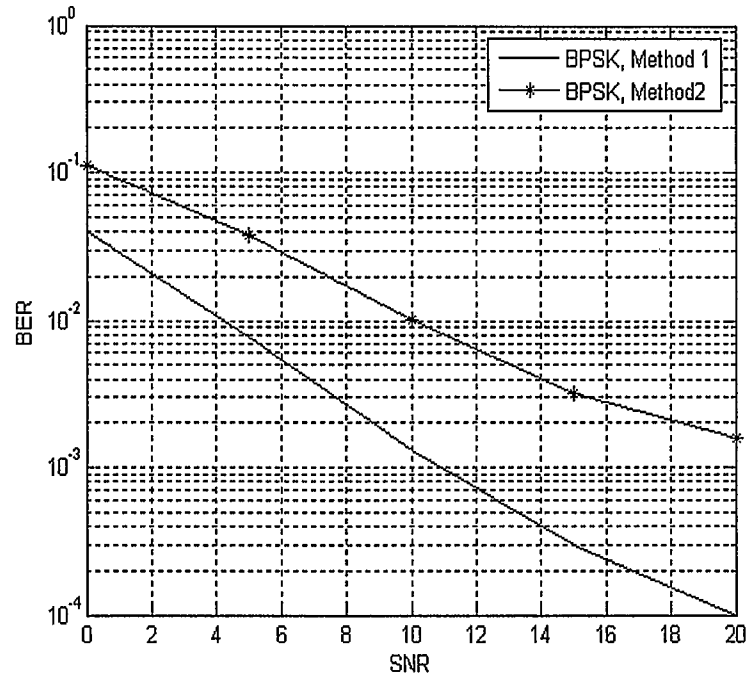


Figure 3.6 Performance Comparison of STBC-DFE with Different Decoding Methods

Using BPSK Modulation(Multi-user Case One)

(2) 8PSK Modulation

The number of feedforward filter taps is 8. The BER vs. SNR performance using the first decoding method is shown in Figure 3.7.

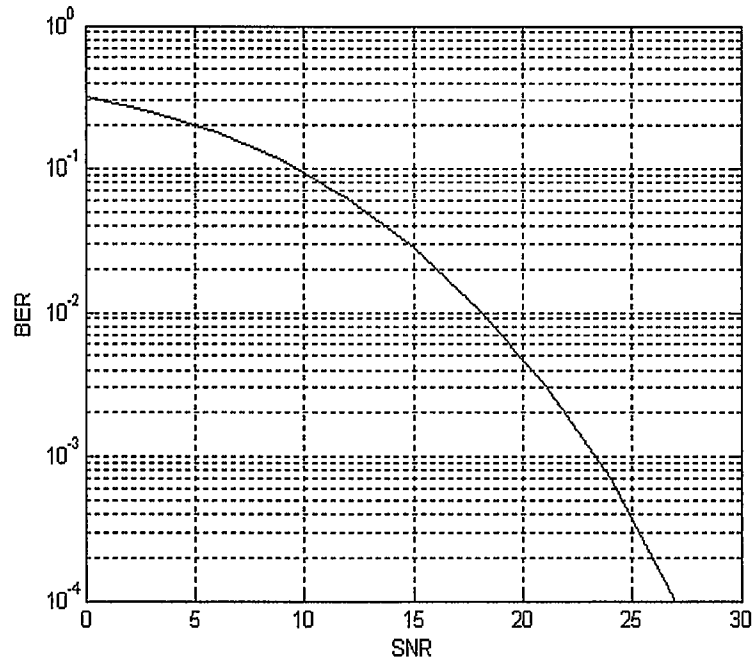


Figure 3.7 BER vs. SNR Performance Using the First Decoding Method
(Multi-userCase One)

3.5.2 STBC-DFE for Multi-User Case Two

(1) BPSK Modulation

In this case, we consider a multi-user system where all the users are ordered and previous and current estimates from lower indexed users are available to higher indexed users. We use band LDL factorization to get the optimum parameters of the feedforward filter and feedback filter of DFE .

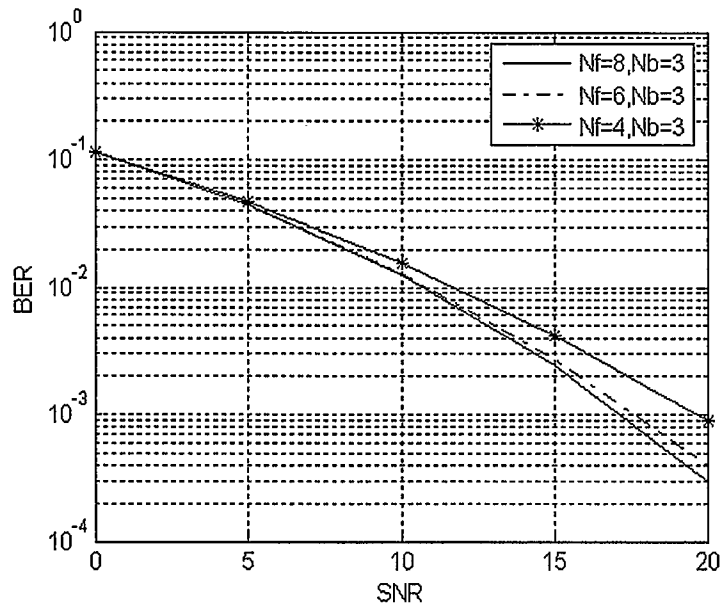


Figure 3.8 Performance Comparison of STBC-DFE with Different Taps Using BPSK modulation (Multi-user Case Two)

Figure 3.8 shows BER vs. SNR performance comparisons of the STBC-DFE schemes with different feedforward filter taps. In Figure 3.8, as the number of feedforward filter taps (N_f) increases from 6 to 8, the performance improvement of the STBC-DFE scheme is limited for all SNR region. Hence, the influence of the taps of feedforward filter for the multi-user case two is limited when the number of taps is greater than 6.

We also compare the performance of the STBC-DFE schemes with the two decoding methods for the multi-user case two. The number of feedforward filter taps is fixed at 8 for both schemes. Figure 3.9 shows that the STBC-DFE scheme with the first decoding method has better performance although the improvement is limited (about 2dB when BER is 10^{-3}). Comparing Figure 3.9 to Figure 3.6, for the multi-user case two, the

performance difference between the two decoding methods is not as much as that for the multi-user case one.

(2) 8PSK Modulation

The number of feedforward filter taps is 8. The BER vs. SNR performance using the first decoding method is shown in Figure 3.10.

Comparing Figure 3.10 with Figure 3.7, the BER performance in multi-user case two is worse than the BER performance in multi-user case one when the same modulation and decoding method are used. It is about 3 dB worse when the BER is 10^{-3} .

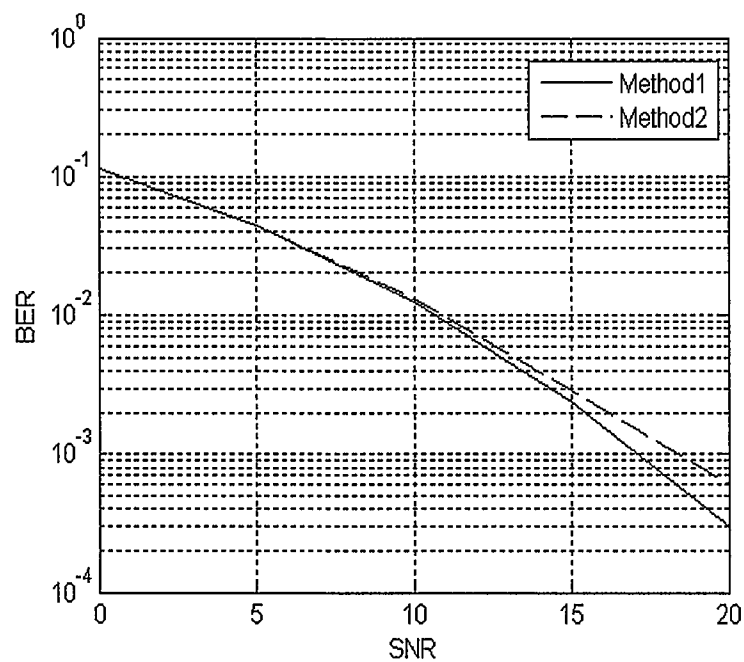


Figure 3.9 Performance Comparison of STBC-DFE with Different Decoding Methods
Using BPSK Modulation (Multi-user Case Two)

From all the above simulation results, we can have the following conclusions: For the multi-user case one, with the increase of the feedforward filter taps, the performance improvement of the STBC-DFE scheme is apparent. While for the multi-user case two, the influence of feedforward filter taps for the STBC-DFE system is limited when the number of the feedforward taps is greater than 6. According to the simulation results, the performance of the STBC-DFE using first decoding method is better. However, the second decoding method can achieve comparable performance with a simple system structure especially for the multi-user case two. Hence, the second decoding method is a good choice for the practical cases in which simple computation has absolute priority.

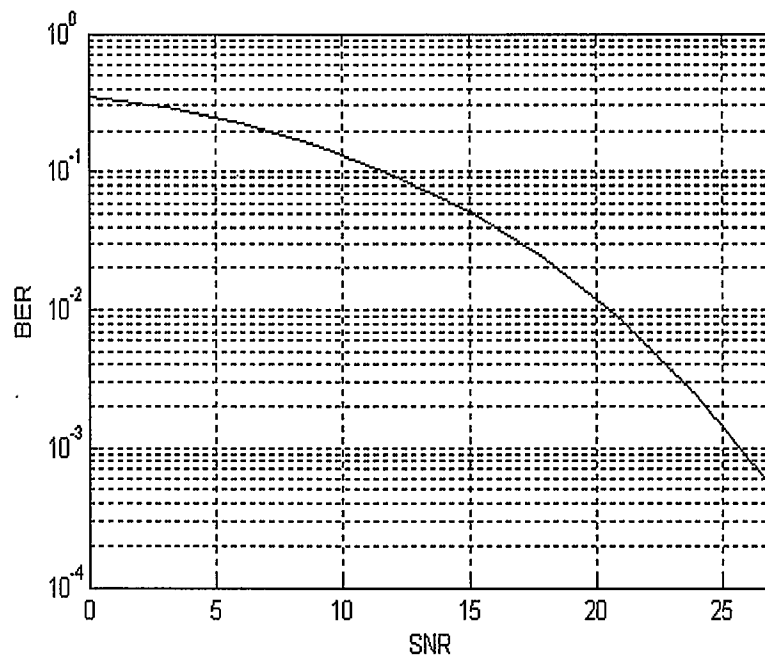


Figure 3.10 BER vs. SNR Performance Using the First Decoding method
(Multi-user Case Two)

3.6 Chapter Summary

In this chapter, space-time coding theory is introduced. In particular, a popular space-time coding method STBC is narrated in details. The elaborate structures of two STBC-DFE schemes are given. In the computer simulations, single-user and multi-user situations are discussed using both BPSK and 8PSK modulation. The simulation results are analyzed and compared. The simulation results of the two STBC-DFE schemes show that these schemes have good performance and acceptable computation load. Therefore, they are potential solutions for next generation wireless communication.

CHAPTER FOUR: STBC-DFE SCHEMES COMBINED WITH CONVOLUTIONAL CODES

In digital mobile channels, the interference usually results from the combination of additive white Gaussian noise (AWGN) and Rayleigh fading. Coded modulation (CM) can efficiently improve transmission quality in communication system. Hence, designing coded modulation system suitable to the two channel characteristics, has practical meaning. When convolutional codes are used in CM, it is called trellis-coded modulation (TCM). In the following content, convolutional coding is introduced first.

4.1 Convolutional Codes

In a convolutional code's encoder, the number of output bits of each k -bit input sequence is n bits. The encoded sequence is related with not only the k -bit input sequence but also the previous $(N-1)$ k -bit sequences. The related code bits are nN . A convolutional code has the following properties:

- 1) The error correction ability increases as N increases; while bit error rate decreases as N increases.
- 2) Normally, k and n are very small, which is suitable for serial transmission and has small time delay.
- 3) When the complexities of the encoders are same, the performance of the convolutional codes is better than that of the block codes.
- 4) The strict mathematics explanation for the relationship between the error correction ability and the structure of a convolutional code, has not been

discovered. Now code selection is mainly dependent on computer searching [41].

4.1.1 Convolutional Codes Generation

In general, a convolutional code is generated through a linear finite-state shift register which consists of K (k -bit) stages and n linear algebraic function generators, as shown in Figure 4.1. For each k -bit input sequence, the output is n -bit. The encoded sequence is related with not only the k -bit input sequence but also the previous $(N-1)$ k -bit sequences. The whole encoding process can be regarded as the convolution of the input sequence and the sequence decided by the mod-2 summers' connections. The name of convolutional code comes from this fact. N is called the constraint length of the convolutional code. The definition of the constraint length is not uniform. In some literature, nN or $(N-1)$ is called the constraint length [41]. Normally, convolutional codes are given in the form (n,k,N) which indicates the convolutional code with code rate $R_c = k/n$.

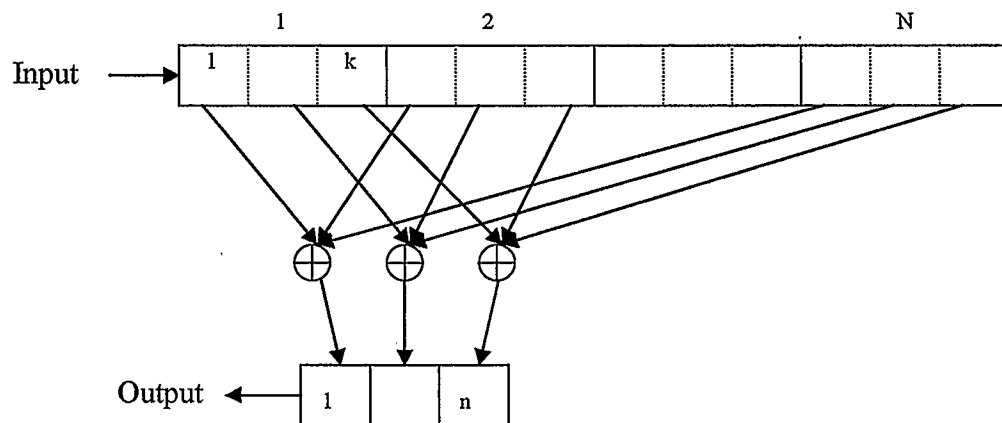


Figure 4.1 General Encoder of Convolutional Codes

4.1.2 Hamming Distance in Convolutional Codes

As we know, Hamming distance and error correction ability are closely related. In code generation, Hamming distance should be as large as possible and the minimum free distance is the measurement of error correction ability.

In convolutional codes, commonly there are two kinds of distance: minimum distance d_{\min} and free distance d_{free} . The minimum Hamming distance among encoded sequences with length nN (N is the constraint length) is called minimum distance d_{\min} . The minimum Hamming distance among encoded sequences with arbitrary length is called free distance d_{free} . As code bit is not used in convolutional codes, taking free distance as the measurement of error correction ability is more reasonable [41]. Generally, d_{\min} and d_{free} are obtained by computer searching. In a Gaussian channel, the convolutional codes with code rate R and free Hamming distance d_{free} , has asymptotic coding gain [42] as follows

$$G = Rd_{\text{free}} \quad (4.1)$$

4.2 Decoding of Convolutional Codes

There are three decoding algorithms for convolutional codes: Viterbi decoding algorithm, sequence decoding algorithm and threshold decoding algorithm. Viterbi and sequence decoding are statistics decoding algorithms; threshold decoding is based on Bernouli Law of Large Number.

1) Maximum Likelihood Decoding Algorithm

Viterbi decoding algorithm is one kind of Maximum Likelihood (ML) decoding algorithm. Hence, here ML decoding theory is first introduced.

In a convolutional code's encoding and decoding system, the decoder receives the output sequence from the channel. Assume all the channel input sequences are equi-probable and Y is the input sequence to decoder. If the condition

$$P[Y/X(M')] \geq P[Y/X(M)] \text{ for } M' \neq M$$

is satisfied, the decoder's output is M' , which will minimize the sequence error rate[43]. The decoder is optimal and called ML sequence decoder. Conditional probability $P[Y/X(M)]$ is called likelihood function. Therefore, the output of ML sequence decoder maximizes the value of likelihood function.

Usually logarithmic likelihood function is more convenient because of two reasons: logarithm is nondecreasing function, the size relationship does not change after logarithm conversion; logarithmic likelihood function has superposition property for received symbols. So the decoding of convolutional codes is to find the path which maximizes the superposition value of the logarithmic likelihood function for a certain received sequence. For a binary channel, assuming $P(1/0)=P(0/1)=P$, L symbols in sequence X are transmitted and there are e symbol errors in the transmission (or e symbols in Y are different from the symbols at the same positions in X), then the Hamming distance between the two sequences is e . The logarithmic likelihood function is

$$\log P[Y/X] = \log [P^e (1-P)^{L-e}] = L \log(1-P) - e \log[(1-P)/P] = -A - B_e$$

For $P < 0.5$, A and B are both positive constants. When the Hamming distance is minimum, the value of logarithmic likelihood function is maximum. That is to say computing the maximum value of the logarithmic likelihood function is equivalent to computing the minimum Hamming distance between the two sequences X and Y . Then, maximum likelihood decoding is to select a path in the tree diagram or the trellis diagram

to minimize the Hamming distance or Euclidean distance between the corresponding decoded sequence and received sequence. Normally, the Hamming distance or Euclidean distance between a possible decoded sequence and the received sequence is called measurement.

2) Viterbi Decoding Algorithm

Viterbi decoding algorithm is one of Maximum Likelihood decoding methods. The decoding trellis for the convolutional codes (2,1,3) is shown in Figure 4.2.

In a convolutional code's trellis, there are $2^{k(N-1)}$ states, each state (or each node) has 2^k incoming paths and 2^k outgoing paths. For convenience, take $k=1$ as an example, the initial state is all-zero. For each path that converges at a common node, the logarithm of each path is summed together. Hence, there are totally two summations for each node. The path with bigger summation value is kept and the other path is discarded, i.e. only one of the two paths survives at each node. As each node has two outgoing paths, the posterior stage has double paths, but after all the value summations of logarithmic function are compared, half of the paths are discarded and the number of survived paths is a constant.

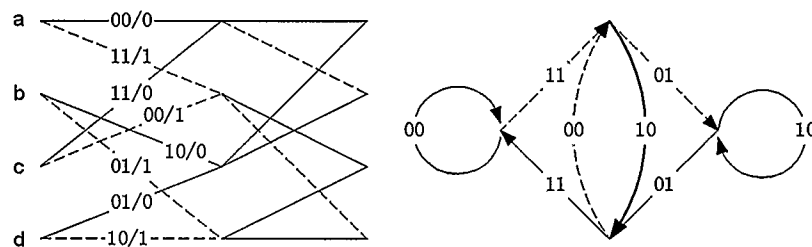


Figure 4.2 Trellis and Status Diagram

In a word, the above decoding process is a “summation-comparison-selection” process, i.e. on each stage the logarithm summation of each path is computed, compared and selected. Sometimes, for two paths, the logarithm summations are same. In this case the survived path will be randomly selected from these two paths. So after comparison on each stage, the number of survived paths reduces 50 percent. Then, through (N-1) selections, there is only one survived path left. This path is the decoding result. When the received sequence is known, this result is most adjacent to the transmitted sequence. This process is shown in Figure 4.2. From the above, we can see Viterbi decoding algorithm’s procedure is not complex and the decoder is forward without feedback. Because for each node on each stage, the summation-comparison-selection process is needed, the encoder’s complexity is proportional to the number of states and increases exponentially as the constraint length N increases. Decoding a L-bit sequence, the total number of decoding operations is $L2^{N-1}$. When $L > N$, $L2^{N-1}$ is much smaller than 2^{L-1} which is the number of decoding operations in Maximum Likelihood decoding algorithm. However, the computation of Viterbi decoding algorithm is still very large because it increases exponentially as the constraint length N increases. As a result, Viterbi decoding algorithm is only used in the convolutional codes with shorter constraint length ($N \leq 10$). Note that actually the above conclusion information is the general information without error. Hence, as long as the error pattern doesn’t exceed the convolutional codes’ error correction ability, the survived paths from one node can correctly assemble together after a certain interval. While it is not determinate how long the interval is and where they assemble, they are relevant to the error pattern. Obviously, in practice, decoding depth

can only be fixed instead of random. The decoding depth N and the number of states 2^{N-1} decide the content needed to be saved, because the 2^{N-1} paths with length N must be saved before the paths' assembling. Only when the path with minimum measurement is decided, can the content in the memorizer be refurbished. Hence, the memorizer's capacity is at least enough for $M \cdot 2^{N-1}$ measurements and paths. The decoding depth N is normally decided through computer simulations and is a compromise between capacity and equipment cost. The decoding depth N is the decoder's constraint length. It is also the decoding time delay generated by decoder. In practice, decoding constraint length is 3 to 5 times of the encoding constraint length. In the computer simulations of this chapter, the convolutional codes (2,1,3) and Viterbi decoding algorithm with decoding constraint length 15 are used.

3) Sequential Decoding Algorithm

Sequential decoding algorithm is proposed before Viterbi decoding algorithm. It is also based on Maximum Likelihood decoding theory. It takes the Hamming distances among paths as the measurements and selects the closer path to the received sequence. Comparing with Viterbi decoding algorithm, sequential decoding algorithm only extends a path with minimum Hamming distance to compare and select instead of extending all possible paths. This algorithm searches in a single path using sequential method. After each transaction, the path with ML probability is selected. If the decision is incorrect, the posterior paths are incorrect. According to the change of path measurement, the decoder can recognize if the path is correct or not. When the decoder recognizes that the path is incorrect, it will search backwards and try other paths till a correct path is found.

4) Threshold Decoding Algorithm

Threshold decoding algorithm is based on set partitioning. When it is used in the decoding of convolutional codes, the convolutional codes are considered as set partitioning codes with decoding constraint length. The decoding theory is based on the concept of orthogonal parity check sum. The basic idea is to compute correction sub-sequences [43]. In general, the convolutional codes, which are suitable to threshold decoding, are usually system codes.

4.3 STBC-DFE Combined with Convolutional Codes

The system structures of STBC-DFE combined with convolutional codes using two decoding methods are shown in Figure 4.3 and Figure 4.4, respectively. In these two figures, each system has an additional part – convolutional codes decoder – compared to the corresponding STBC-DFE system without convolutional codes.

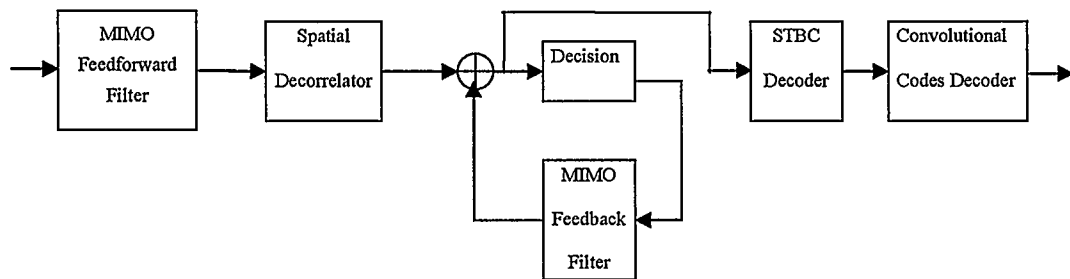


Figure 4.3 System Structure of STBC-DFE combined with Convolutional Codes
(using the first decoding method)

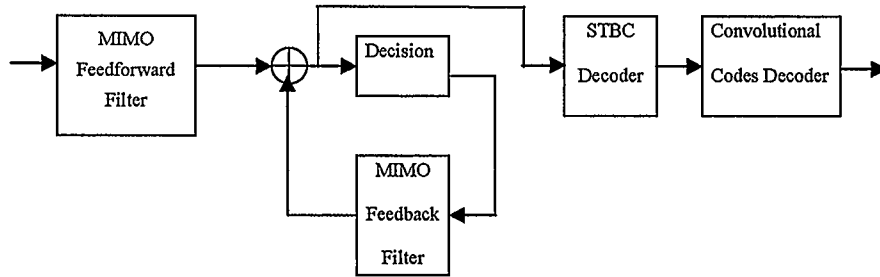


Figure 4.4 System Structure of STBC-DFE combined with Convolutional Codes
(using the second decoding method)

4.4 Computer Simulations and Analysis

We simulate the convolutional coded STBC-DFE systems with the two decoding methods for two multiple-user cases in the Typical Urban channel where the channel memory equals 3. The power delay profile is given in Table 3.5 in chapter three. Two transmit antennas and two receive antennas are used and each antenna transmits at half the transmit power of the single transmit antenna case. The number of feedback filter taps is 3, which is equal to the channel memory. The number of the feedforward filter taps is fixed at $N_f=8$. BPSK modulation is used. The convolutional code (2,1,3) and Viterbi decoding algorithm are used. The decoding constraint length is five times of the encoding constraint length, i.e. 15.

4.4.1 STBC-DFE Combined with Convolutional Code for Multi-user Case One

In Figure 4.5, the system using the first decoding method has much better performance than the system using the second decoding method. Comparing Figure 4.5 with Figure 3.6 one page 30, we found the performance difference between two decoding methods is

enlarged in Figure 4.5. In Figure 3.6, when BER is 10^{-2} , the difference is 5.5 dB. While in Figure 4.5, when BER is 10^{-2} , the difference is almost 15 dB. This is due to the property of convolutional codes: for any two systems, when the addition of convolutional codes do have benefits, convolutional codes usually add more coding gain to the system which already has better performance. As a result, the performance difference between the two systems becomes larger. The reason is: for better system (usually in terms of BER vs. SNR performance), there are fewer errors to control, therefore convolutional codes can add more coding gain. From chapter three, we know the first decoding method has better performance. Hence, with the addition of convolutional codes, although both systems have performance improvement, the system using the first decoding method improves a lot more than the system using the second decoding method.

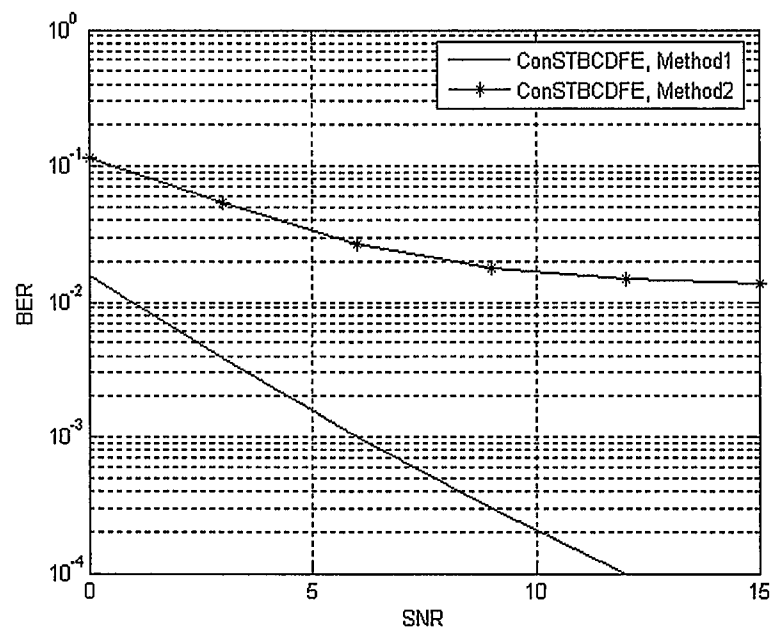


Figure 4.5 Performance Comparison of the System Combining Convolutional Codes and STBC-DFE using Different Decoding Methods (Multi-user Case One)

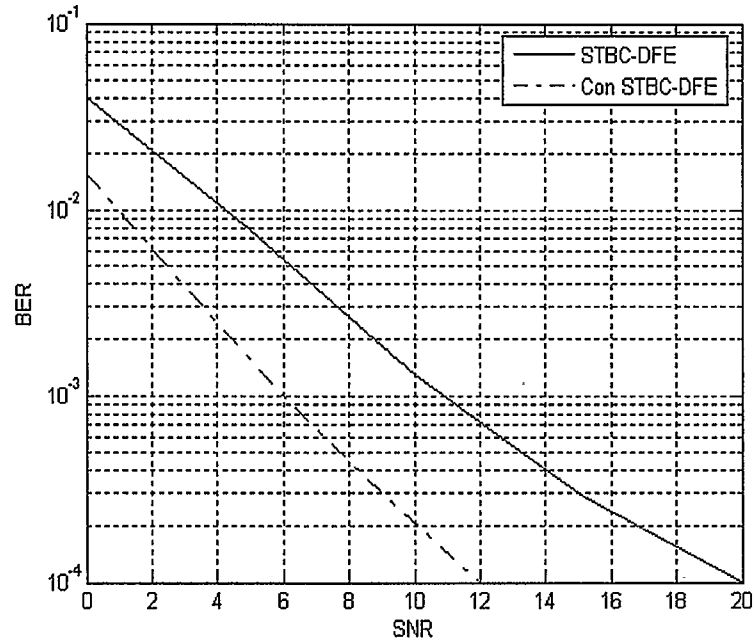


Figure 4.6 Performance Comparison of the STBC-DFE Systems with and without Convolutional Codes (Multi-user Case One)

In Figure 4.6, the first decoding method is used for the two systems. In this figure, the STBC-DFE system combined with convolutional codes greatly outperforms the STBC-DFE system without convolutional codes. The gain is 5dB when BER is 10^{-3} . When BER is 10^{-4} , the gain is 8dB.

4.4.2 STBC-DFE Combined with Convolutional Codes for Multi-user Case Two

Compared to the case one, the system using the first decoding method also has much better performance than the system using the second decoding method. Comparing Figure 4.7 and Figure 3.9 on page 33, similar to multi-user case one, we have the finding that the

performance difference between two decoding methods is enlarged in Figure 4.7. In Figure 3.9, when BER is 10^{-3} , the difference is less than 1dB. While in Figure 4.7, the difference is 7.5dB when BER is 10^{-3} . And from Figure 4.5 and Figure 4.7, the difference between the two decoding methods in multi-user case two is much less than that in multi-user case one.

From all the above simulation results, we have a conclusion that convolutional codes can provide additional coding gain to the STBC-DFE system. When convolutional codes are combined with the STBC-DFE system using the first decoding method, the performance improvement is very large (about 8 dB when BER is 10^{-4} in single-user situation).

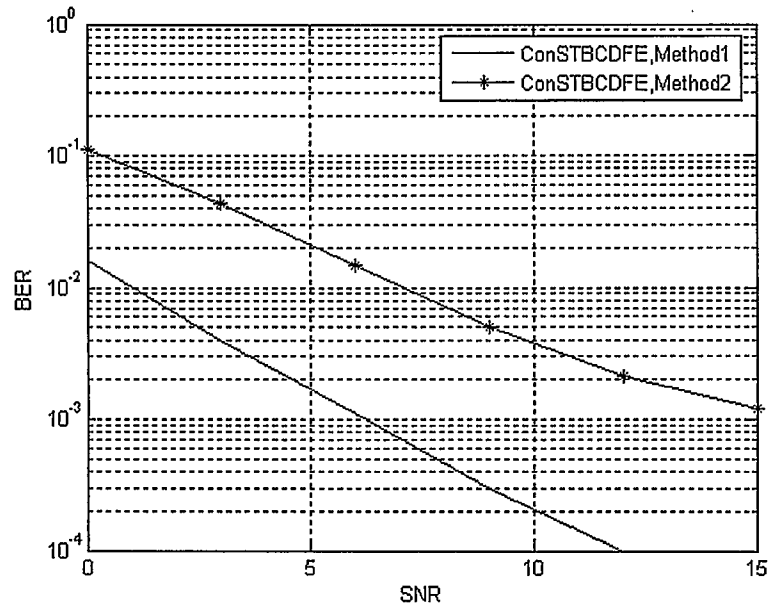


Figure 4.7 Performance Comparison of the System Combining Convolutional Codes and STBC-DFE using Different Decoding Methods (Multi-user Case Two)

4.5 Chapter Summary

In this chapter, the encoding and decoding of convolutional codes are described in detail. The combination structures of STBC-DFE and convolutional codes are given. Computer simulation results of STBC-DFE combined with convolutional codes under two multi-user situations are given and analyzed. These simulation results are also compared with the STBC-DFE system without convolution codes. The system with convolutional codes has much better performance, which proves the STBC-DFE system can obtain additional coding gain with the addition of convolutional codes.

CHAPTER FIVE: PERFORMANCE COMPARISON BETWEEN STBC-OFDM AND STBC-DFE

Comparing with wire communications, the distinguished advantage of wireless communications is: they eliminate the limitation from wire and can meet the communication requirements from people everywhere at any moment, so they develop at a very fast speed. There are many problems in wireless communications, such as limited frequency spectrum and detrimental channel situations. Among these problems, one prominent problem is multi-path time delay expansion which limits the improvement of data transmission rate. The reason is: if data transmission rate is higher than coherence bandwidth (coherence bandwidth is determined by time delay expansion and is the inverse of time delay expansion in general), signals will suffer from serious distortion, transmission quality will decrease to a large extent.

Orthogonal frequency division multiplexing (OFDM) is a special multi-carrier modulation technology and highly efficient data transmission method [7]. The fundamental idea is: a high data rate sequence is separated and transmitted in multiple orthogonal sub-carriers, which greatly decreases the symbol rate in sub-carriers and increases the symbol duration. Hence, OFDM has stronger resistibility to time delay expansion and reduces inter-symbol interference (ISI). Normally, a guard interval is added before an OFDM signal. If the guard interval is bigger than the channel time delay expansion, ISI can be eliminated totally. The difference between OFDM and the other multiple carrier transmission technologies is that OFDM permits the superposition of sub-carriers' frequency spectrum and if sub-carriers are orthogonal to each other, data

information can be extracted from the superposed sub-carriers. OFDM permits the superposition of sub-carriers' frequency spectra, therefore it is a highly effective modulation technology [8, 10]. OFDM has good resistibility to narrow band interference, because narrow band interference only affects very few parts of the sub-carriers in OFDM; and for frequency selective channels, frequency diversity can be obtained by using error-control codes in the sub-carriers.

As OFDM has the above advantages, it is a potential solution for high data rate transmission [44]. But in the early OFDM system, the subsidiary carrier sequence is generated by frequency generator and all subsidiary carriers need to be accurately synchronous for coherent reception, so when the number of sub-channels is very large, the system is very complex and expensive. To simplify frequency generator sequence, in 1971, Weinstein and Ebert proposed to use Discrete Fourier Transform Algorithm (DFT) [7], for example, the dedicated hardware- Fast Fourier Transform (FFT) circuit, to realize all the modulation and demodulation functions in OFDM system, which mitigates the strict synchronization limitation between frequency generator sequence and local carriers in correlative receiver and is a theory preparation for OFDM digitalization design. As very large-scale integration (VLSI) develops fast, dedicated high speed and precision FFT chips and general digital signal processing (DSP) chips using software to realize FFT, have come forth and the prices are low. These new technologies make it possible to realize OFDM. In 1980's, people mainly investigated how to use OFDM in high speed modulators and demodulators. From 1990's, OFDM technology has been explored in linear frequency modulation channels with emphasis on the applications of wideband data transmission in wireless situations. Currently, it is a trend to use OFDM technology

in high data rate communications, such as European Digital Audio Broadcast (DAB) and Digital Video Broadcast (DVB). OFDM can also be used in wire communications, for example, Asymmetrical Digital Subscriber Loop (ADSL). Now due to the fast development of digital signal processing technology, OFDM has attracted extensive attention because of its anti-ISI effectiveness and high data rate.

5.1 Orthogonal Frequency Division Multiplexing Theory

Frequency division multiplexing transforms signals from serial to parallel and divides the signal frequency spectrum into many sub-channels, then modulates each sub-channel signal and sends the summation of all the sub-channel signals. In the receiver, at first the received signals are sampled, then serial-to-parallel transformed and demodulated, at last the signals are parallel-to-serial transformed to get the recovered signals.

Based on frequency division multiplexing theory, OFDM limits each carrier to be orthogonal to all the other carriers. If the carrier frequency f_0, \dots, f_{M-1} in sub-channels satisfy the following relationship:

$$f_k = f_0 + k/T_b, \quad k=0,1,\dots,M-1$$

where f_0 is transmit frequency, T_b is unit code duration time.

Assume carrier's unit signal is:

$$P_k(t) = \begin{cases} \cos(2\pi f_k t), & 0 \leq t < T_b \\ 0 & \text{otherwise} \end{cases} \quad (5.1)$$

Then

$$\int P_n(t)P_m(t)dt = \begin{cases} T_b & m = n \\ 0 & m \neq n \end{cases} \quad (5.2)$$

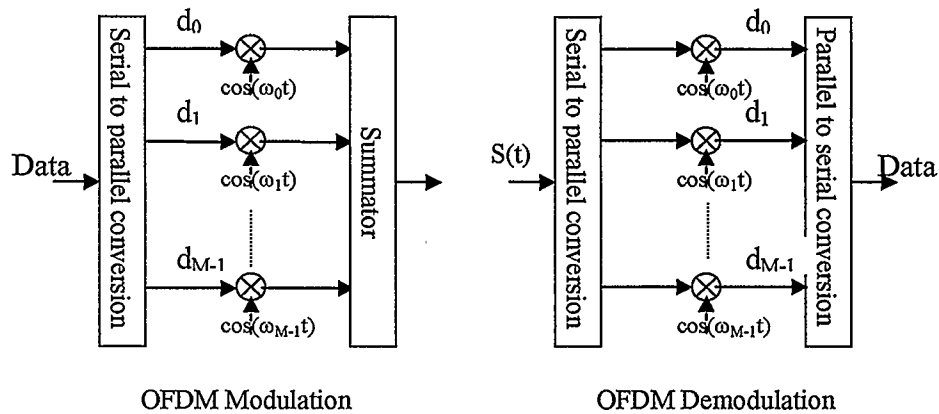


Figure 5.1 OFDM Modulation/Demodulation

Therefore, these carrier signals are orthogonal to each other. OFDM system's demodulation theory is shown in Figure 5.1.

OFDM's frequency spectrum is shown in Figure 5.2. In Figure 5.2, there is a wider guard band between the adjacent sub-channels' frequency spectrums in Frequency Division Multiplexing (FDM), while the adjacent sub-channels' frequency spectrums superpose in OFDM. Therefore, OFDM improves frequency spectrum efficiency while remaining the characteristics of FDM.

5.2 Fast Fourier Transform for OFDM Modulation and Demodulation

As shown in Figure 5.1, OFDM signal $S(t)$ can be expressed as

$$s(t) = \sum_{k=0}^{M-1} d_k \cos(\omega_k t) \quad (5.3)$$

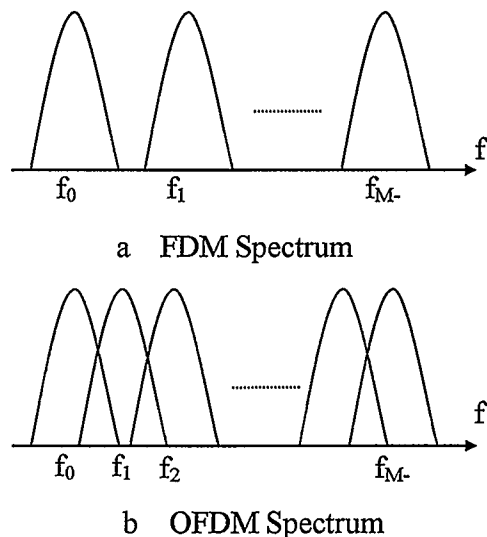


Figure 5.2 FDM Spectrum and OFDM Spectrum

Assume a data sequence $\vec{D} = \{d_0, \dots, d_{M-1}\}$, Inverse Discrete Fourier Transform (IDFT)

\vec{D} to complex vector $\vec{S} = \{S_0, \dots, S_{M-1}\}$,

$$S_n = \sum_{k=0}^{M-1} d_k e^{j \frac{2\pi n k}{M}} = \sum_{k=0}^{M-1} d_k e^{j \frac{2\pi f_k t_n}{M}} \quad (n=0,1,\dots, M-1) \quad (5.4)$$

where $f_k = \frac{k}{M\Delta t}$, $t_n = n\Delta t$, $\cos(t)|_{t=nT_b} = \sum_{k=0}^{M-1} d_k \cos(2\pi f_k t_n) = R_e[S_n]$, ($n=0,1,\dots, M-1$).

Hence, the real part of vector $\vec{S} = \{S_0, \dots, S_{M-1}\}$ is sent to low pass filter, then a signal $S(t)$, which is similar to FDM signal, can be obtained. Applying Inverse Fast

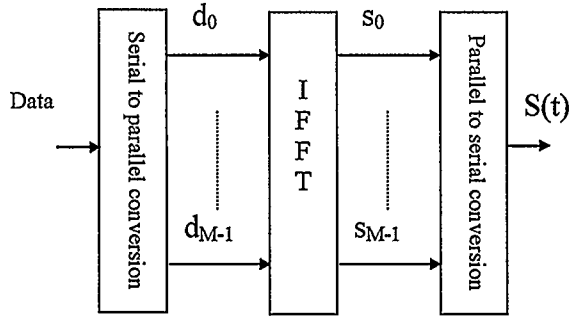


Figure 5.3 OFDM Modulation Using IFFT

Fourier Transform to IDFT vector $\vec{D} = \{d_0, \dots, d_{M-1}\}$, OFDM modulation is achieved, as shown in Figure 5.3. In the receiver, the received signals are sampled at double rate.

The sample signal is:

$$y(n) = \sum_{k=0}^{M-1} d_k \cos\left(\frac{2\pi nk}{2M}\right) \quad (n=0,1,\dots,2M-1)$$

When there is no distortion in channels, in the receiver, DFT $2N$ sample points as follows:

$$\begin{aligned} \gamma(k) &= \sum_{n=0}^{2M-1} y(n) W_{2M}^{nk} = \sum_{n=0}^{2M-1} \sum_{l=0}^{M-1} d_l \cos\left(\frac{2\pi ln}{2M}\right) W_{2M}^{nk} = \frac{1}{2} \sum_{n=0}^{2M-1} \sum_{l=0}^{M-1} d_l (W_{2M}^{ln} + W_{2M}^{-lk}) W_{2M}^{nk} \\ &= \frac{1}{2} \sum_{n=0}^{2M-1} d_l \sum_{l=0}^{M-1} (W_{2M}^{(l+k)n} + W_{2M}^{(k-l)n}) W_{2M}^{nk} \quad k = 0,1,2,\dots,2M-1 \end{aligned} \quad (5.5)$$

$$\text{For } \sum_{n=0}^{2M-1} W_{2M}^{(l+k)n} = \begin{cases} 2M, & l+k = 2Mq, q = 0, \pm 1, \dots \\ 0 & \text{otherwise} \end{cases}$$

$$\text{and } \sum_{n=0}^{2M-1} W_{2M}^{(k-l)n} = \begin{cases} 2M, & k-l = 2Mq, q = 0, \pm 1, \dots \\ 0 & \text{otherwise} \end{cases},$$

we have

$$\gamma(k) = \begin{cases} 2Md_0, & k=0 \\ Md_k, & k=1, 2, \dots, M-1 \end{cases} \quad (5.6)$$

Therefore, DFT of the sampled signals are transmitted signals. Using FFT to realize the DFT of the sampled signals, is OFDM demodulation, as shown in Figure 5.4.

From what has been said, OFDM modulation and demodulation can be realized by IDFT and DFT respectively. FFT and IFFT are effective algorithms for computing DFT and IDFT. So far there has been a great improvement in FFT algorithm. The software for FFT algorithm is very effective and rounded and hardware based on FFT develops very fast. Utilizing FFT to realize OFDM modulation and demodulation, can efficiently improve data rate with reasonable cost.

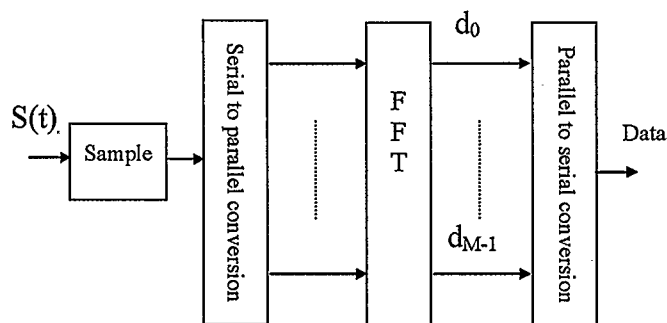


Figure 5.4 OFDM Modulation Using FFT

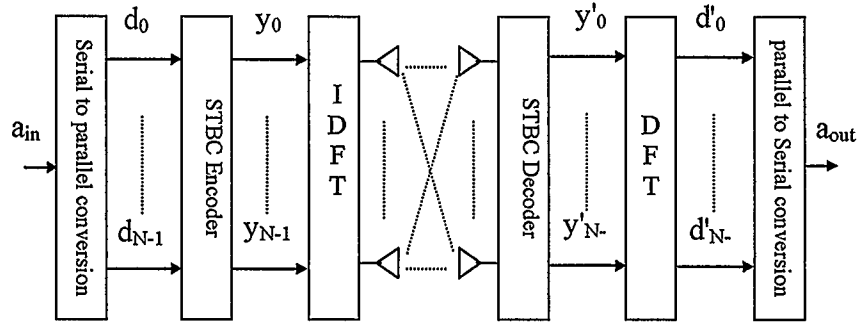


Figure 5.5 STBC-OFDM System

The advantages of OFDM are very prominent and its inherent disadvantages can be corrected and mitigated by some new effective technologies. Spatial diversity technology can efficiently improve the quality of wireless communications. Combining spatial diversity technology and OFDM, can further the transmission quality in wireless fading channels [45-47].

5.3 STBC-OFDM System

The combination of STBC and OFDM can further improve the performance. The structure of STBC-OFDM system is shown in Figure 5.5. In this figure, there are n transmit antennas and m receive antennas in the STBC-OFDM system. The signal transmission is according to the orthogonal theory of STBC (the detailed description is in chapter 3).

5.4 Computer Simulations and Analysis

The Typical Urban channel, where the channel memory equals 3, is used. The power delay profile is given in Table 3.5 in chapter three. Two transmit antennas and two receive antennas are used and each antenna transmits at half the transmit power of the single transmit antenna case. The number of feedback filter taps and feedforward filter taps are 3 and 8 respectively. BPSK modulation is used. In Figure 5.6, for low SNR region (0 to 7.5 dB), the performance of STBC-DFE system combined with convolutional codes is even better than that of the STBC-OFDM system; for high SNR region, the performance of STBC-DFE system combined with convolutional codes is worse than that

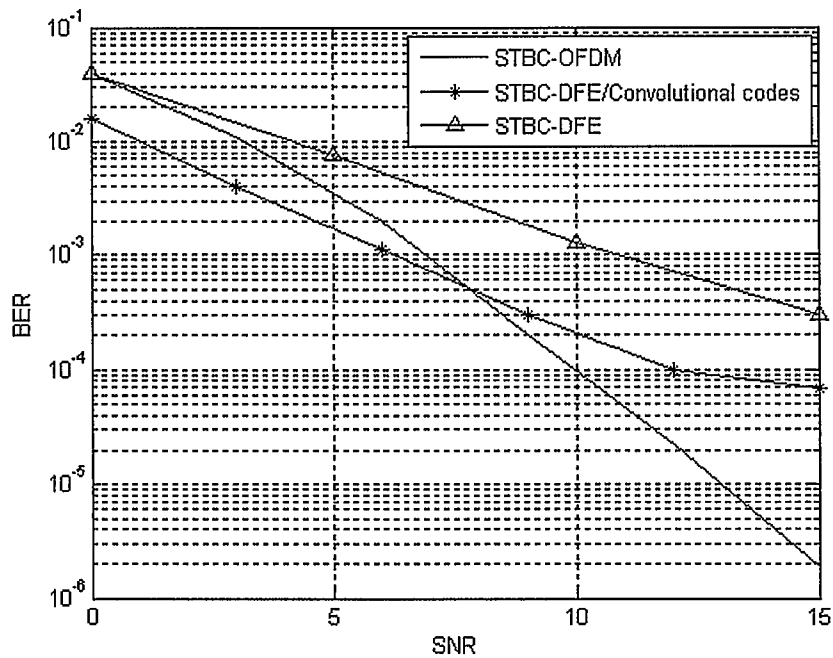


Figure 5.6 Performance Comparison among Three Systems

Using the First Decoding Method

of the STBC-OFDM system, but it is still comparable (about 2dB worse when BER is 10^{-4}). The simulation results further prove that convolutional codes is a very good anti-error method, which is a big advantage in low SNR situations. While anti-error is not the most important issue in high SNR situations, the advantage of convolutional codes is not as evident as the inherent advantages of OFDM.

5.5 Chapter Summary

In this chapter, the modulation and demodulation of OFDM system are introduced. How to use FFT and IFFT to realize the modulation and demodulation is also described. The structure of STBC-OFDM system and the simulation results are given. Those results are compared with the STBC-DFE systems with and without convolutional codes and prove that the concatenation of convolutional codes and STBC-DFE provides a good optional solution for multi-path transmission.

CHAPTER SIX: CONCLUSIONS

Comprehensively considering the computer simulations and analysis in the previous chapters, some conclusions can be obtained as follows:

1. From the simulation results of DFE using block iterative normalized LMS algorithm in a SISO system, we know that BINLMS is not a very effective estimation algorithm and can not satisfy practical communication requirements.
2. The elaborate structures of two STBC-DFE schemes are given. In the computer simulations, two multi-user cases are discussed using both BPSK and 8PSK modulation. The simulation results shows that those two STBC-DFE schemes have good performance and acceptable complexity. Hence, they are potential solutions for the next generation mobile communication.
3. The combination structures of STBC-DFE and convolutional codes are given. Computer simulation results of these systems under two multi-user situations are given. These simulation results are compared with the STBC-DFE system without convolution codes. The STBC-DFE system with convolutional codes has much better performance. This indicates convolutional codes can provide great coding gain to the STBC-DFE system.
4. The structure of STBC-OFDM system and the simulation results are given. The results are compared with the STBC-DFE systems with and without convolutional codes. Note that for low SNR region, the performance of the STBC-DFE system combined with convolutional codes, is even better than that of the well-known STBC-OFDM. Therefore, for low SNR, the combination of convolutional codes and STBC-DFE is a good choice for multi-path transmission.

In this thesis, the decision feedback equalizer (DFE) in multiple-input multiple-output Rayleigh fading channels, is investigated and the above conclusions are obtained. In the investigation, there are still some problems remaining. From the author's point of view, there are two potential directions for this research. One direction is we can combine Turbo codes with STBC-DFE to further improve the system performance. The other is using DFE in frequency domain instead of in time domain. And if more practical channel condition is used, i.e. comprehensively considering Doppler shift, time delay, channel capacity, multi-path interference and frequency selective fading, the simulation results and corresponding conclusions will be more useful.

REFERENCES

1. Al-Mashouq, Khalid A. and Reed, I.S., "The Use of Neural Nets to Combine Equalization with Decoding for Severe Intersymbol Interference Channels", *IEEE Trans. on Neural Networks*, vol. 5, issue. 6, Nov. 1994, Page(s):982- 988
2. Benedetto, S.E., *Digital Transmission Theory*, Prentice-Hall, Inc., 1987
3. Vahid Tarokh, Nambi Seshadri, A.R.Calderbank, "Space-Time Codes for High Data Rate Wireless Communication: Performance Criterion and Code Construction", *IEEE Trans. on Information Theory*, vol. 44, no.2, March 1998, pp. 744-765
4. J.L.Massey, "Coding and modulation in digital communications," *Proceedings of Int. Zurich Seminar on Digital Comm.*, Zurich, Switzerland, March 1974, pp. E2(1) -E2(4)
5. G. Umgerboeck, "Channel coding with multilevel/phase signals," *IEEE Trans. Inform. Theory*, vol.28, January 1982, pp.55-67
6. E. Biglieri, D.Divsalar, P.J. McLane, and M. K. Simon, *Introduction to Trellis-Coded Modulation with Applications*. New York: Macmillan, 1991
7. Weinstein S. B, Ebert P. M., "Data Transmission by Frequency Division Multiplexing Using the Discrete Fourier Transform", *IEEE Trans. on Communications*, vol. 19, no. 15, Oct. 1971
8. L. J. Cimini, Jr., "Analysis and simulation of a digital mobile channel using orthogonal frequency division multiplexing", *IEEE Trans. on Communications*, vol. 33, July 1985, pp. 665-675

9. B. Hirosaki, "An analysis of automatic equalizers for orthogonally multiplexed QAM systems", *IEEE Trans. on Communications*, vol. 28, no. 1, Jan. 1980, pp. 73-83
10. B. Hirosaki, "An orthogonally multiplexed QAM system using the discrete Fourier transform", *IEEE Trans. on Communications*, vol. 29, no. 7, July 1981, pp. 982-989
11. I. Kalet, "The multitone channel", *IEEE Trans. on Communications*, vol. 37, no. 2, February 1989, pp. 119-124
12. P. S. Chow, J. M. Cioffi and J. A. C. Bingham, "A practical discrete multitone transceiver loading algorithm for data transmission over spectrally shaped channels", *IEEE Trans. on Communications*, vol. 43, no. 4, April 1995, pp. 773-775
13. T. J. Willink and P. H. Wittke, "Optimization and performance evaluation of multicarrier transmission", *IEEE Trans. Information Theory*, vol. 43, no. 2, March 1997, pp. 426-440
14. S.U.H. Qureshi, "Adaptive equalization," *Proceedings of IEEE*, vol.73, no.9, Sept.1985, pp. 1349-1387
15. J. G. Proakis, *Digital Communications*, 3rd ed. McGraw-Hill Inc.: New York, NY,1995.
16. R. Price. "Nonlinearly feedback-equalized PAM vs capacity for noisy filter channels". *Proceedings of the IEEE International Conference on Communications*, 1972, pp 22-26

17. J. Salz. "Optimum Mean-Square Decision Feedback Equalization". *Bell System Technical Journal*, vol. 52, no.8, Oct. 1973, pp.1341
18. D.I. Messerschmitt., "A Geometric Theory of Intersymbol Interference. Part I: Zero-Forcing and Decision-Feedback Equalization". *Bell System Technical Journal*, vol. 52, no.9, pp.1483-1519
19. C.A. Belfiore and J.H. Park Jr. "Decision Feedback Equalization". *Proceedings of IEEE*, vol.67, no.8, August 1979, pp.1143-1156
20. N. Zervos and I. Kalet. "Optimized decision feedback equalization versus optimized Orthogonal Frequency Division Multiplexing for high-speed data transmission over the Local Cable Network", *Proceedings of IEEE International Conf. on Communications*, Boston, June 1989, pp. 1080-1085
21. J.M. Cioffi, G.P. Dudevoir, M. V. Eyuboglu, and G.D. Forney. "MMSE Decision-Feedback Equalizers and Coding - Part I: Equalization Results". *IEEE Trans. on Communications*, vol. 43, no. 10, Oct.1995, pp 2582-2594
22. R.G. Gallager. "*Information Theory and Reliable Communication*". Wiley, New York, 1968
23. G. D. Fomey Jr., "Maximum-likelihood sequence estimation of digital sequences in the presence of intersymbol interference," *IEEE Trans. Inform. Theory*, vol. 18, no.3, May 1972, pp. 363-378

24. S. U. Qureshi and E. E. Newhall, "An adaptive receiver for data transmission over time-dispersive channels," *IEEE Trans. Inform. Theory*, vol.19, July 1973, pp. 448-457
25. D. D. Falconer and F. R. Magee Jr., "Adaptive channel memory truncation for maximum-likelihood sequence estimation," *Bell System Technical Journal*, vol. 52, Nov. 1973, pp. 1541-1562
26. C. T. Beare, "The choice of desired impulse response in combined Linear-Viterbi algorithm equalizers," *IEEE Trans. on Communications*, vol.36, Aug. 1978, pp. 1301-1337
27. W. U. Lee and F. S. Hill, "A maximum-likelihood sequence estimator with decision-feedback equalization," *IEEE Trans. on Communications*, vol.25, Sept. 1977, pp. 971-979
28. J. C. S. Cheung and R. Steele, "Soft decision feedback equaliser for CPM signals," *Proceedings of the IEEE International Conference on Communications*, Denver, USA, June 1991, vol. 3, pp. 1469-1473
29. M. V. Eyuboglu and S.U.H. Qureshi, "Reduced-state sequence estimation with set partitioning and decision feedback," *IEEE Trans. on Communications*, vol.36, Jan.1998, pp.13-20
30. A. Duel-Hallen and C. Heegard, "Delayed decision-feedback sequence estimation," *IEEE Trans. on Communications*, vol. 37, May 1989, pp. 428-436

31. M. Stojanovic, J. Catipovic and J. Proakis, "Reduced complexity simultaneous beam forming and equalization for underwater acoustic communications", *Proceedings of IEEE Oceans' Conference*, Victoria, Canada, Oct.1993, pp.426-431
32. P.Monsen, "Theoretical and measured performance of a DFE modem on a fading multipath channel," *IEEE Trans. on Communications*, vol. 25, Oct. 1977, pp.1144-1153
33. D. Duttweiler, J. Mazo and D. Messerschmitt, "Error propagation in decision-feedback equalizers," *IEEE Trans. Inform. Theory*, vol. 20, July 1974, pp.490-497
34. John F. Doherty and Richard James Mammone, "An adaptive algorithm for stable decision-feedback filtering," *IEEE Trans. Circuits and System-II*, vol.40, no.1, January 1993, pp.1-9
35. Rappaport Theodore S, "*Wireless Communications: Principles and Practice*," Prentice Hall, 1996
36. A. Naguib, V. Tarokh, N.Seshadri, and A. R. Calderbank, "A space-time coding modem for high-data-rate wireless communications," *IEEE Journal on Selected Areas in Communications*, vol.16, Oct. 1998, pp. 1459-1477
37. Naofal Al-Dhahir, Ali H.Sayed, "The finite-length multi-input multi-output MMSE-DFE", *IEEE Trans. on Signal Processing*, vol. 48, no. 10, Oct. 2000, pp. 2921-2936
38. Siavash M. Alamouti, "A simple transmit diversity technique for wireless communications", *IEEE Journal on Selected Areas in Communications*, vol.16, 1998, pp1451-1458.

39. Bertrand M. Hochwald, and Thomas L. Marzetta, "Unitary Space-Time Modulation for Multiple-Antenna Communications in Rayleigh Flat Fading", *IEEE Trans. on Information Theory*, vol. 46, March 2000, pp. 543-564
40. Naofal Al-Dhahir, Ayman F. Naguib, and A. R. Calderbank, "Finite-length MIMO decision feedback equalization for space-time block-coded signals over multipath-fading channels", *IEEE Trans. Vehicular Technology*, vol. 50, no. 4, Jul. 2001, pp. 1176-1182
41. Yutaka Yasuda, Kanshiro Kashika and Yasuo Hirata, "High-Rate Punctured Convolutional Codes for Soft Decision Viterbi Decoding", *IEEE Trans. On Communication*, vol. 32, no. 3, Mar. 1984, pp. 315-319
42. A. T. Viterbi and J. K. Omura, *Principles of Digital Communications*, McGraw-Hill, 1979
43. G.C.Clark and J.B.Cain, "Error Correction Codes in Digital Communication", Springer, June 1981
44. Nee Richard Van., *OFDM Wirless Multimedia Communications*, Artech House, Jan., 2000
45. Liu Z., Giannakis G.B., Barbarossa S., Scaglione A., "Transmit Antennae Space-Time Block Coding for Generalized OFDM in The Presence of Unknown Multipath", *IEEE Journal on Selected Areas in Communications*, vol. 19, July 2001, pp.1352 -1364

46. Yi Gong, Letaief K.B., "Space-Frequency-Time Coded OFDM for Broadband Wireless Communications", *Proceedings of IEEE Global Telecommunications Conference*, San Antonio, USA, Nov. 2001, vol. 1, pp. 519 -523

47. Agrawal D., Tarokh V., Naguib A., Seshadri N., "Space-Time Coded OFDM for High Data-Rate Wireless Communication over Wideband Channels", *Proceedings of IEEE Vehicular Technology Conference*, Ottawa, Canada, May 1998, vol. 3, pp. 2232-2236